Eur. Phys. J. C (2016) 76:576
DOI 10.1140/epjc/s10052-016-4413-1

THE EUROPEAN PHYSICAL JOURNAL C

Regular Article - Theoretical Physics

Quarkonium Contribution to Meson Molecules

E. Cincioglu[1,a], **J. Nieves**[2], **A. Ozpineci**[3], **A. U. Yilmazer**[1]

[1] Department of Physics Engineering, Ankara University, Ankara, Turkey
[2] Instituto de Física Corpuscular (IFIC) Centro Mixto CSIC-Universidad de Valencia, Institutos de Investigación de Paterna, 46071 Valencia, Spain
[3] Department of Physics, Middle East Technical University, Ankara, Turkey

Received: 13 June 2016 / Accepted: 30 September 2016 / Published online: 25 October 2016

Abstract Starting from a molecular picture for the $X(3872)$ resonance, this state and its $J^{PC} = 2^{++}$ heavy-quark spin symmetry partner [$X_2(4012)$] are analyzed within a model which incorporates possible mixings with $2P$ charmonium ($c\bar{c}$) states. Since it is reasonable to expect the bare $\chi_{c1}(2P)$ to be located above the $D\bar{D}^*$ threshold, but relatively close to it, the presence of the charmonium state provides an effective attraction that will contribute to binding the $X(3872)$, but it will not appear in the 2^{++} sector. Indeed in the latter sector, the $\chi_{c2}(2P)$ should provide an effective small repulsion, because it is placed well below the $D^*\bar{D}^*$ threshold. We show how the 1^{++} and 2^{++} bare charmonium poles are modified due to the $D^{(*)}\bar{D}^{(*)}$ loop effects, and the first one is moved to the complex plane. The meson loops produce, besides some shifts in the masses of the charmonia, a finite width for the 1^{++} dressed charmonium state. On the other hand, $X(3872)$ and $X_2(4012)$ start developing some charmonium content, which is estimated by means of the compositeness Weinberg sum rule. It turns out that in the heavy-quark limit, there is only one coupling between the $2P$ charmonia and the $D^{(*)}\bar{D}^{(*)}$ pairs. We also show that, for reasonable values of this coupling, leading to $X(3872)$ molecular probabilities of around 70–90 %, the X_2 resonance destabilizes and disappears from the spectrum, becoming either a virtual state or one being located deep into the complex plane, with decreasing influence in the $D^*\bar{D}^*$ scattering line. Moreover, we also discuss how around 10–30 % charmonium probability in the $X(3872)$ might explain the ratio of radiative decays of this resonance into $\psi(2S)\gamma$ and $J/\psi\gamma$. Finally, we qualitatively discuss within this scheme, the hidden bottom flavor sector, paying a special attention to the implications for the X_b and X_{b2} states, heavy-quark spin–flavor partners of the $X(3872)$.

[a] e-mail: elif.cincioglu@gmail.com

1 Introduction

The $X(3872)$ state was first observed by the Belle collaboration [1] in the $B^{\pm} \to J/\psi\pi^+\pi^- K^{\pm}$ channel as a narrow peak and was confirmed by various other experiments [2–5]. The averaged mass of $X(3872)$ is 3871.69 ± 0.17 MeV, which is only 0.16 MeV below the $D^0\bar{D}^{*0}$ threshold and the full width is less than 1.2 MeV [6]. In addition, the LHCb experiment determined its J^{PC} quantum numbers as 1^{++} [7]. The properties of $X(3872)$ turned out to be difficult to reconcile with a $c\bar{c}$ state in a quark potential model picture [8,9]. Alternative theoretical models have been proposed to understand its structure. One of the popular descriptions of $X(3872)$ is as a molecular state consisting of a D and a $\bar{D}^*$ [10–17].

One of the puzzling observations about $X(3872)$ is the ratio of its decays into final states with isospin-0 and isospin-1. The ratio of the decay fractions of $X(3872)$ into $J/\psi\pi^+\pi^-$ and into $J/\psi\pi^+\pi^-\pi^0$ final states was first measured by Belle [18] to be:

$$\frac{Br(J/\psi\pi^+\pi^-\pi^0)}{Br(J/\psi\pi^+\pi^-)} = 1.0 \pm 0.4 \pm 0.3. \tag{1}$$

For the same ratio, BABAR has obtained $1.0 \pm 0.8 \pm 0.3$ [19]. Later Belle announced the updated results of the measurements for the reaction $J/\psi\pi^+\pi^-\pi^0$, and thus the accepted combined result from Belle and BABAR is 0.8 ± 0.3 [20]. The decays into final states with two and three pions proceed through virtual ρ and ω mesons, respectively. Considering the phase space differences between the ρ and ω mesons, the production amplitude ratio is found to be [21]

$$\left|\frac{A(J/\psi\rho)}{A(J/\psi\omega)}\right| = 0.26 \pm 0.07. \tag{2}$$

Such a large isospin violation arises naturally in the molecular picture due to the mass difference between the $D^0\bar{D}^{*0}$ and D^+D^{*-} components in the $X(3872)$ wave function [17,22],

and the remarkable proximity of the resonance to the $D^0\bar{D}^{0*}$ threshold.

Other interesting $X(3872)$ measurements are its radiative decays. The ratio of the branching fractions into final states with a photon and a J/ψ or a $\psi(2S)$ has been measured as [23,24]:

$$R_{\psi\gamma} = \frac{Br(X \to \psi(2S)\gamma)}{Br(X \to J/\psi\gamma)} = 2.46 \pm 0.64 \pm 0.29. \qquad (3)$$

One of the first works where the radiative decays of the $X(3872)$ was studied within an effective field theory framework was carried out in [25]. There, the $X(3872) \to \psi(2S)\gamma$ reaction was studied and some qualitative conclusions were drawn. It was argued that the decay should receive a contribution from long-distance physics, involving the propagation of intermediate heavy charm mesons ($D^0\bar{D}^{*0} - hc$), and short-distance dynamics, whose contribution is encoded in a contact operator. The $\chi_{c1}(2P)$ state contributed to the latter operator, through $D\bar{D}^* \to \chi_{c1}(2P) \to \psi(2S)\gamma$. The relative importance of these two types of contributions was unknown, though it was shown in [25] that the angular distributions of the decay products can be used to distinguish between them.

There were claims [26] that within the molecular picture, such a large ratio cannot be naturally explained. This ratio can be, however, accommodated assuming that there is a charmonium admixture in the molecular state [27–30]. Thus for instance, an enhanced decay of the $X(3872)$ into $\psi(2S)\gamma$ compared to $J/\psi\gamma$, and fully compatible with a predominantly molecular nature of $X(3872)$ was found in Ref. [30], where a phenomenological study allowing for both a molecular as well as a compact component of the $X(3872)$ was carried out. Actually, an admixture of 5–12 % of a $\bar{c}c$ component was sufficient to explain the data [30]. This charmonium admixture is also favored by the production rate of $X(3872)$ in the $p\bar{p}$ collisions which is about 1/20 of the rate of $\psi(2S)$. This production rate can easily be explained if one assumes that the $c\bar{c}$ component of $X(3872)$ is approximately 5 % [31].

The validity of the claim of Ref. [30] was critically reviewed in Ref. [32] from an effective field theory (EFT) point of view. There, it was concluded, contrary to earlier claims, that radiative decays do not allow one to draw conclusions on the nature of $X(3872)$. Actually, the findings of Ref. [30] were qualitatively confirmed, and in addition it was pointed out that the observed ratio is not in conflict with a predominantly molecular nature of the $X(3872)$. The study of Ref. [32] suggests that, for radiative decays of the $X(3872)$, short-range contributions are of similar importance as their long-range counter parts.

In the heavy-quark limit, an EFT to describe the $X(3872)$ and also other possible $D^{(*)}\bar{D}^{(*)}$ molecules has been proposed in [33,34]. At very low energies, the leading order (LO) interaction between the $D^{(*)}\bar{D}^{(*)}$ mesons can be described just in terms of contact-range potentials, which are constrained by heavy-quark spin symmetry (HQSS). Pion exchange and particle coupled channel[1] effects are conjectured to be sub-leading, and they are not considered at LO, within the scheme advocated in [33,35], where it is assumed that HQSS is respected in the interactions, but broken by the heavy–light meson masses. This scheme, in principle, should make sense for loosely bound molecules, as their binding is smaller than the meson mass splittings, and it requires the use of ultraviolet (UV) regulators sufficiently small to prevent violations of HQSS. In [33,35], it is argued on general grounds that expected coupled-channel effects should be suppressed by the square of the ratio of the light scale over the coupled-channel momentum scale, which in the charm sector is around 500–700 MeV. Moreover, the consideration of coupled channels induced a strong dependence on the UV regulator [33,35], which would require the inclusion of additional counter-terms to compensate for, increasing thus the number of undetermined low energy constants (LECs).

Within the molecular description of the $X(3872)$, among others, the existence of a X_2 [$J^{PC} = 2^{++}$] S-wave $D^*\bar{D}^*$ bound state was predicted in the EFT approach of Refs. [33,34], with a binding energy similar to that of the $X(3872)$ ($M_{X_2} - M_{X(3872)} \approx M_{D^*} - M_D \approx 140$ MeV). Both the $X(3872)$ and the X_2 would have partners in the bottom sector [36],[2] which we will call X_b and X_{b2}, respectively, with masses approximately related by $M_{X_{b2}} - M_{X_b} \approx M_{B^*} - M_B \approx 46$ MeV. States with 2^{++} quantum numbers exist as well as spin partners of the 1^{++} states in the spectra of the conventional heavy quarkonia and tetraquarks. However, the mass splittings would only accidentally be the same as the fine splitting between the vector and pseudoscalar charmed mesons.

Some exotic hidden charm sectors have also been studied recently on the lattice [37–41], and evidence for the $X(3872)$ from $D\bar{D}^*$ scattering on the lattice has been found [38]. The 2^{++} sector has not been exhaustively addressed yet, though a state with these quantum numbers and a mass of $(m_{\eta_c} + 1041 \pm 12)$ MeV$= (4025 \pm 12)$ MeV, close to the value predicted in Refs. [33,34], was reported in Ref. [37], though the calculations were performed with a pion mass $\simeq 400$ MeV. There exists also a feasibility study [42] of future lattice QCD (LQCD) simulations, where the EFT approach of Refs. [33,34] was formulated in a finite box.

Despite the theoretical predictions on the existence of the X_2, X_b and X_{b2} states, none of these hypothetical particles has been observed so far. This negative result could be

[1] We do not refer to charge channels, but rather to the mixing among the $D\bar{D}$, $D\bar{D}^*$, $D^*\bar{D}^*$ pairs in a given IJ (isospin and spin) sector.

[2] In Ref. [36], the bottom and charm sectors are connected by assuming the bare couplings in the four-meson interaction Lagrangian to be independent of the heavy-quark mass.

because the current experiments are not yet sensitive enough or due to the non-existence of these states. Nevertheless, they are being and will be searched for in current and future experiments such as BESIII, LHCb, CMS, Belle-II and PANDA.

The HQSS EFT approach of Refs. [33,34] does not consider possible mixings between molecular heavy–light meson–antimeson and quarkonium states. However, in the LQCD simulation carried out in Ref. [38], it was needed to consider both $c\bar{c}$-charmonium and $D\bar{D}^*$-molecular type interpolating fields to find a signature[3] of the $X(3872)$. As discussed above, the presence of $c\bar{c}$ components in the $X(3872)$ seems also to be required to explain the experimental value for the ratio of radiative branching fractions $R_{\psi\gamma}$, quoted in Eq. (3). Moreover, the charmonium $\chi_{c1}(2P)$ state, which would have the same quantum numbers 1^{++} as the $X(3872)$, has not been found yet.

The charmonium admixture in a molecular picture of the $X(3872)$ has been studied, among others, in Refs. [30,31,43]. In Ref. [31], direct interactions between the D and $\bar{D}^*$ mesons are supposed to play a marginal role, being the coupling to the $c\bar{c}$ core more important in creating the $X(3872)$ than the direct $D\bar{D}^*$ attraction, which is assumed to be independent of the isospin as well as of the heavy-quark masses. The strength of the $D\bar{D}^*$ attraction is estimated to be barely strong enough to make a weakly bound state by looking at the experimental masses of the isovector $Z_b(10610)$ and $Z_b(10650)$ resonances, placed very close to the $B\bar{B}^*$ and $B^*\bar{B}^*$ thresholds, respectively. This rationale might be incorrect since the $D\bar{D}^*$ interaction for isospin 1 is suppressed in the large N_C (number of colors) counting with respect to that in the isoscalar sector. A non-relativistic constituent quark model is used in Ref. [43], and two- and four-quark configurations are coupled using the phenomenological $^3P_0$ model. Finally, the approach of Ref. [30] is based on phenomenological hadron Lagrangians and the quark model results of Ref. [10], where it is proposed that the $X(3872)$ is a $D^0\bar{D}^{*0}$ hadronic resonance stabilized by admixtures of $\omega J/\psi$ and $\rho J/\psi$. These works neither made use of HQSS, nor address the dynamics of possible heavy-quark spin–flavor partners of the $X(3872)$ states. There exist however, some preliminary results [44], obtained within the quark model of Ref. [43], about the possible existence of heavy-quark spin–flavor partners of the $X(3872)$.

It is therefore timely and relevant to extend the HQSS model of Refs. [33,34] to incorporate quarkonium degrees of freedom, and their possible mixings with the molecular components. This is the objective of the present work, where we will make use of HQSS and the experimental ratio $R_{\psi\gamma}$ to constrain the interaction of the $D^{(*)}\bar{D}^{(*)}$ pairs with the $2P$ charmonia. (Due to the closeness of their masses, the charmonium admixture in the $X(3872)$ should correspond to the $2P$ $c\bar{c}$ states.) We will also study the effects of non-zero quarkonium components on the predictions for the X_2, X_b and X_{b2} states. We will show that even small mixings between charmonium and molecular components in the X_2 state might explain why it has not been observed yet. In the hidden bottom sector, however, we will see how despite the changes induced by the quarkonium admixtures, it might be reasonable to expect that both X_b and X_{b2} resonances should be real QCD states, which might be observed in the short future.

In Ref. [45] and working in the strict heavy-quark limit, the degeneracy of the X_2 and $X(3872)$ states was confirmed as a robust result with respect to the inclusion of the one-pion exchange interaction between the $D^{(*)}$ mesons. There, it is shown that this is true if all relevant partial waves as well as particle channels which are coupled via the pion-exchange potential are taken into account. Beyond the heavy-quark limit and treating non-perturbatively the pions, in [45] it is predicted, contrary to the findings of Refs. [33,42] obtained with perturbative pions, a significant shift of the X_2 mass and width of the order of 50 MeV. The increase of the X_2 binding energy is only viewed in [45] as a qualitative result. However, the conclusion on the broadening of the X_2 is claimed in that work as a reliable prediction, since it is argued there that is related to unitarity. We think these findings have to be interpreted with some caution. First, one should bear in mind that the UV cutoffs used in [45] are much larger (around a factor of 2) than those considered in the approach of Refs. [33,42]. Thus some extra HQSS breaking corrections, beyond those due to the heavy–light meson masses, are accounted for in [45], which have indeed relevance in the numerical results. Such corrections are largely cut in Refs. [33,42], and it is not clear whether they should be considered or not, and given the poor experimental status, it is difficult to disentangle among both approaches. Second, the hadronic D-wave $X_2 \to D\bar{D}$ and $X_2 \to D\bar{D}^*$ two-body decays, driven via one pion exchange, were predicted in [42] to be smaller altogether than 5 MeV. There, large contributions from highly virtual pions carrying large momenta, which lie outside the range of applicability of the EFT as proposed in Refs. [33,42] were found. Such contributions were further suppressed in [42] by including an extra form factor in the vertices involving virtual pions. As can be seen in Table 1 of the latter reference, X_2 widths as large as 30 MeV could be obtained without including this extra form factor. Thus, it is not surprising that values of around 50 MeV were found in [45] for the width of this resonance since there, as mentioned above, much larger UV regulators were used.

In the following, we will use the EFT as conjectured in Refs. [33,42] and will neglect pion exchange and coupled-

[3] There, it was also found that the effect of the $J/\psi\omega$ channel is irrelevant for the dynamics of the $X(3872)$. In that exploratory work, isospin breaking effects were not considered, and thus the resonance reported in [38] was purely isoscalar.

channel effects in this preliminary study of the interplay between quark and meson-molecular degrees of freedom. However, one should consider also the possibility of a broad X_2 state from a purely molecular picture, as found in the approach pursued in Ref. [45], which nevertheless would be also affected by the consideration of the quark degrees of freedom discussed in the present work.

This paper is organized as follows. In Sect. 2, and within a framework suited to implement HQSS constraints, we introduce the heavy-quark fields and their interactions, including those responsible for the mixing between meson–meson pairs and P-wave quarkonium states. Also in this section, the $2P \to 1S, 2S$ charmonium radiative transitions are studied (Sect. 2.4). In the next section, Sect. 3, the procedure used to obtain unitarized amplitudes, from the HQSS interactions introduced in the previous section, is described. A special attention (Sect. 3.2) is paid to a non-perturbative re-summation based on the solution of a renormalized Lippmann–Schwinger equation (LSE). In Sect. 4, some general properties of the poles of the unitarized amplitudes and the compositeness condition, which will serve us to quantify the importance of the molecular components in the resonances, are discussed. Specific formulas for the two-channel problem relevant to study the 1^{++} and 2^{++} hidden charm or bottom meson molecules are given in the first part of Sect. 5. Numerical results on the influence of the quarkonium components in the properties of the $X(3872)$, $X_2(4012)$, X_b and X_{b2} meson molecules are presented and discussed in Sects. 5.1, 5.2 and 5.3. In Sect. 5.1, a numerical study of the $X(3872) \to J/\psi\gamma$ and $\psi(2S)\gamma$ transitions, based on Sect. 2.4 and Ref. [32], is presented and used to constrain the charmonium content in the $X(3872)$. The most relevant findings of this work are summarized in Sect. 6, and finally, the properties of the 1^{++} and 2^{++} hidden charm and bottom poles discussed in the previous sections, but calculated with a different UV regulator are collected in Appendix A.

2 LO effective Lagrangians

2.1 HQSS fields

We use the matrix field $H^{(Q)}$ $[H^{(\bar{Q})}]$ to describe the combined isospin doublet of pseudoscalar heavy-mesons $P_a^{(Q)} = (Q\bar{u}, Q\bar{d})$ $[P^{(\bar{Q})a} = (u\bar{Q}, d\bar{Q})^t]$ fields and their vector HQSS partners $P_a^{*(Q)}$ $[P^{*(\bar{Q})a}]$ (see for example [46]),

$$H_a^{(Q)} = \frac{1+\not{v}}{2}\left(P^{*(Q)}_{a\mu}\gamma^\mu - P_a^{(Q)}\gamma_5\right), \quad v\cdot P_a^{*(Q)} = 0,$$
$$H^{(\bar{Q})a} = \left(P^{*(\bar{Q})a}_{\mu}\gamma^\mu - P^{(\bar{Q})a}\gamma_5\right)\frac{1-\not{v}}{2}, \quad v\cdot P^{*(\bar{Q})a} = 0. \tag{4}$$

The matrix field H^c $[H^{\bar{c}}]$ annihilates P $[\bar{P}]$ and P^* $[\bar{P}^*]$ mesons with a definite velocity v. Under a parity transformation we have

$$H^{(Q,\bar{Q})}(x^0,\vec{x}) \to \gamma^0 H^{(Q,\bar{Q})}(x^0,-\vec{x})\gamma^0, \qquad v^\mu \to v_\mu. \tag{5}$$

The field $H_a^{(Q)}$ $[H^{(\bar{Q})a}]$ transforms as a $(2,\bar{2})$ $[(\bar{2},2)]$ under the heavy spin $\otimes$ SU(2)$_V$ isospin symmetry [46], this is to say:

$$H_a^{(Q)} \to S_Q\left(H^{(Q)}U^\dagger\right)_a, \quad H^{(\bar{Q})a} \to \left(UH^{(\bar{Q})}\right)^a S_{\bar{Q}}^\dagger. \tag{6}$$

Their hermitian conjugate fields are defined by

$$\bar{H}^{(Q)a} = \gamma^0[H_a^{(Q)}]^\dagger\gamma^0, \quad \bar{H}_a^{(\bar{Q})} = \gamma^0[H^{(\bar{Q})a}]^\dagger\gamma^0, \tag{7}$$

and they transform as [46]:

$$\bar{H}^{(Q)a} \to \left(U\bar{H}^{(Q)}\right)^a S_Q^\dagger, \quad \bar{H}_a^{(\bar{Q})} \to S_{\bar{Q}}\left(\bar{H}^{(\bar{Q})}U^\dagger\right)_a. \tag{8}$$

The definition for $H_a^{(\bar{Q})}$ also specifies our convention for charge conjugation, which is $\mathcal{C}P_a^{(Q)}\mathcal{C}^{-1} = P^{(\bar{Q})a}$ and $\mathcal{C}P^{*(Q)}_{a\mu}\mathcal{C}^{-1} = -P^{*(\bar{Q})a}_\mu$, and thus it follows that

$$\mathcal{C}H_a^{(Q)}\mathcal{C}^{-1} = c\,H^{(\bar{Q})at}\,c^{-1}, \quad \mathcal{C}\bar{H}^{(Q)a}\mathcal{C}^{-1} = c\,\bar{H}_a^{(\bar{Q})t}\,c^{-1} \tag{9}$$

with c the Dirac space charge conjugation matrix satisfying $c\gamma_\mu c^{-1} = -\gamma_\mu^t$, and t denotes the matrix transpose operation.

A heavy-quark–antiquark bound state, characterized by the radial number n, the orbital angular momentum l, the spin s and the total angular momentum J, is denoted by $n\,^{2s+1}l_J$. Parity and charge conjugation are given by $P = (-1)^{l+1}$, $C = (-1)^{l+s}$. If spin dependent interactions are neglected it is natural to describe the spin singlet $n\,^1l_{J=l}$ and the spin triplet $n\,^3l_{J=l-1,l,l+1}$ by means of a single multiplet $\hat{J}(n,l)$. For $l=0$, when the triplet $s=1$ collapses into a single state with total angular momentum $j=1$, this is readily realized by adopting the description [47]

$$\hat{J} = \frac{1+\not{v}}{2}\left(\psi_\mu\gamma^\mu - \gamma_5\eta\right)\frac{1-\not{v}}{2}. \tag{10}$$

Here v^μ denotes the four-velocity associated to the multiplet $\hat{J}$; ψ_μ and η are the spin 1 and spin 0 components respectively; the radial quantum number has been omitted. Notice that the multiplet $\hat{J}$ does not have indices related to light flavors.

The even parity P-wave quarkonium multiplet of states are described by the matrix field [48] ($\epsilon_{0123} = +1$):

$$J^\mu = \frac{1+\not{v}}{2}\left(\chi_2^{\mu\alpha}\gamma_\alpha + \frac{i}{\sqrt{2}}\epsilon^{\mu\alpha\beta\gamma}\chi_{1\gamma}v_\alpha\gamma_\beta + \frac{1}{\sqrt{3}}\chi_0(\gamma^\mu - v^\mu) + h^\mu\gamma_5\right)\frac{1-\not{v}}{2} \tag{11}$$

with $J_\mu v^\mu = 0$. The $\chi_2^{\mu\alpha}$, χ_1^μ, χ_0 and h^μ fields annihilate $\chi_{QJ}(nP)$ and $h_Q(nP)$ quarkonium states, with $J^{PC} = 0^{++}, 1^{++}, 2^{++}$ and 1^{+-}, respectively. Note that the spin two field is symmetric, traceless and orthogonal to v^μ, as $\chi_{1\mu}$ and h_μ. Under parity and charge conjugation symmetries, the matrix field J^μ transforms as follows:

$$J^\mu(x^0,\vec{x}) \overset{P}{\to} \gamma^0 J_\mu(x^0,-\vec{x})\gamma^0, \qquad v^\mu \overset{P}{\to} v_\mu, \tag{12}$$

$$J^\mu \overset{C}{\to} c J^{\mu t} c. \tag{13}$$

The hermitian conjugate field $\bar{J}_\mu$ is defined as

$$\bar{J^\mu} = \gamma^0 J^{\mu\dagger}\gamma^0, \tag{14}$$

and under heavy-quark/antiquark rotations, we have

$$J_\mu \to S_Q J_\mu S_{\bar{Q}}^\dagger, \qquad \bar{J}_\mu \to S_{\bar{Q}} \bar{J}_\mu S_Q^\dagger. \tag{15}$$

2.2 $P^{(*)}\bar{P}^{(*)} \to P^{(*)}\bar{P}^{(*)}$ scattering

At very low energies, the interaction between a heavy and anti-heavy meson can be accurately described just in terms of a contact-range potential. Pion exchange effects turn out to be sub-leading [33,35]. The LO Lagrangian respecting HQSS reads [49]

$$\begin{aligned}\mathcal{L}_{4H} = {} & C_A \,\mathrm{Tr}\left[\bar{H}^{(Q)a} H_a^{(Q)}\gamma_\mu\right]\mathrm{Tr}\left[H^{(\bar{Q})a}\bar{H}_a^{(\bar{Q})}\gamma^\mu\right] \\ & + C_A^\tau \,\mathrm{Tr}\left[\bar{H}^{(Q)a}\vec{\tau}^{\,b}_{\ .a} H_b^{(Q)}\gamma_\mu\right]\mathrm{Tr}\left[H^{(\bar{Q})c}\vec{\tau}^{\,d}_{\ .c}\bar{H}_d^{(\bar{Q})}\gamma^\mu\right] \\ & + C_B \,\mathrm{Tr}\left[\bar{H}^{(Q)a} H_a^{(Q)}\gamma_\mu\gamma_5\right]\mathrm{Tr}\left[H^{(\bar{Q})a}\bar{H}_a^{(\bar{Q})}\gamma^\mu\gamma_5\right] \\ & + C_B^\tau \,\mathrm{Tr}\left[\bar{H}^{(Q)a}\vec{\tau}^{\,b}_{\ .a} H_b^{(Q)}\gamma_\mu\gamma_5\right] \\ & \times \mathrm{Tr}\left[H^{(\bar{Q})c}\vec{\tau}^{\,d}_{\ .c}\bar{H}_d^{(\bar{Q})}\gamma^\mu\gamma_5\right]\end{aligned} \tag{16}$$

with $\vec{\tau}^{\,b}_{\ .a}$ the element (a,b) [row, column] of the Pauli matrices in isospin space, and $C_{A,B}^{(\tau)}$ light flavor independent LECs, which are also assumed to be heavy flavor independent and have dimensions of E^{-2}. Note that in our normalization the heavy or anti-heavy meson fields, $H^{(Q)}$ or $H^{(\bar{Q})}$, have dimensions of $E^{3/2}$ (see [50] for details). This is because we use a non-relativistic normalization for the heavy mesons, which differs from the traditional relativistic one by a factor $\sqrt{M_H}$. For later use, the four LECs that appear in Eq. (16) are rewritten into C_{0A}, C_{0B} and C_{1A}, C_{1B} which stand for the LECs in the isospin $I = 0$ and $I = 1$ sectors, respectively. The relation between both sets reads

$$C_{0\phi} = C_\phi + 3C_\phi^\tau, \qquad C_{1\phi} = C_\phi - C_\phi^\tau, \quad \text{for } \phi = A, B. \tag{17}$$

2.3 $Q\bar{Q}\, n^{2s+1}P_J$ quarkonium–$P^{(*)}\bar{P}^{(*)}$ transition

There is only one HQSS consistent term describing the LO interaction of the $n^{2s+1}P_J$ quarkonium states with the $P^{(*)}\bar{P}^{(*)}$-pairs [51],

$$\begin{aligned}\mathcal{L}_{HHQ\bar{Q}} = {} & \frac{\mathrm{d}}{2}\,\mathrm{Tr}[H^{a(\bar{Q})}\bar{J}_\mu H_a^{(Q)}\gamma^\mu] \\ & + \frac{\mathrm{d}}{2}\,\mathrm{Tr}[\bar{H}^{a(Q)} J_\mu \bar{H}_a^{(\bar{Q})}\gamma^\mu].\end{aligned} \tag{18}$$

This expression accounts for the fact that the two heavy–light mesons are coupled to the heavy–heavy state in S-wave, and therefore the matrix elements do not depend on their relative momentum. Thanks to HQSS, the same coupling controls the interaction of heavy–light mesons both with the three χ states and also with the h one. Another way to see that the interaction term is unique is as follows. To describe the S-wave molecular state, instead of using the basis in which the meson–antimeson pair are coupled to a definite total spin state $|j_{P^{(*)}} j_{\bar{P}^{(*)}} I J\rangle$, with I and J the total isospin and spin of the system, one can choose a different basis in which the heavy and light quarks are independently coupled to definite spins, and the whole system is combined to make the definite spin of the whole state. The elements of such basis are of the form $|(s_Q s_l) I J\rangle$, where $s_Q = 0, 1$ ($s_l = 0, 1$) is the spin of the heavy (light) quark–antiquark pair, and I the isospin of the configuration of the light degrees of freedom. Only isoscalar S-wave molecular states will be relevant for this discussion. The possible transitions between isoscalar molecular and the quarkonia states can be described in terms of the matrix elements of the form (for simplicity, we drop out the isospin index)

$$\langle n^{2s+1} l_{J'}|H^{\mathrm{QCD}}|(s_Q s_l) J\rangle = \delta_{J,J'}\delta_{s,s_Q}\langle nl||H^{\mathrm{QCD}}||s_l\rangle \tag{19}$$

where we have made use of rotational invariance and of HQSS, which guaranties that the spin of the heavy-quark subsystem s_Q is conserved. Using charge conservation, it can also be shown that the matrix element with $s_l = 0$ is zero. Indeed, charge conjugation in the molecular states is given by $(-1)^{s_l+s_Q}$, which together with the action of this symmetry, $(-1)^{1+s}$, on the P-wave quarkonium states implies that only the $s_l = 1$ matrix element is different from zero.[4]

The parameter d in Eq. (18) is an unknown LEC, with dimensions of $E^{-1/2}$. It might depend on the radial quantum number n, and it should be fitted to experimental data or be determined otherwise. Moreover, for a consistent treatment of mesons with two heavy quarks, $1/m_Q$ corrections should also be included [47], breaking the heavy-quark symmetry. This leads to a possible dependence of the d LEC on the heavy flavor configuration. Other parameters which are introduced into the model by the inclusion of the quarkonium degrees of freedom are the masses of these new states.

[4] One can also argue that since s_Q and J are conserved, the remaining angular momentum, $\vec{J} - \vec{s}_Q$ should also be conserved. In the molecular state it corresponds to s_l (since $L = 0$ in the molecule), in the charmonium state $\vec{J} - \vec{s}_Q$ corresponds to $L = 1$. Hence, conservation of $\vec{J} - \vec{s}_Q$ implies that only the $s_l = L = 1$ matrix element is non-zero.

Expressed in terms of the individual fields, the interaction Lagrangian of Eq. (18) reads

$$\begin{aligned}\mathcal{L}_{HHQ\bar{Q}} = &-\sqrt{2}d\Big[-\sqrt{2}\chi_1^{\dagger\eta}\left(P\bar{P}^*_\eta - P^*_\eta\bar{P}\right)\\ &-\sqrt{3}\chi_0^\dagger\left(P\bar{P} + \frac{1}{3}P^*_\eta\bar{P}^{*\eta}\right)\\ &+ h^{\dagger\eta}\left(P\bar{P}^*_\eta + P^*_\eta\bar{P}\right)\\ &+ i\epsilon_{\alpha\mu\rho\eta}v^\alpha h^{\dagger\mu}P^{*\rho}\bar{P}^{*\eta} + 2\chi_2^{\dagger\rho\eta}P^*_\rho\bar{P}^*_\eta\Big] + h.c.\end{aligned} \tag{20}$$

where $P^{(*)}\bar{P}^{(*)}$ annihilates an isospin zero two-meson state, normalized to 1. For instance in the case of charmed mesons, the field combination would be

$$|00> = -\frac{1}{\sqrt{2}}\left(D^{0(*)}\bar{D}^{0(*)} + D^{+(*)}D^{-(*)}\right). \tag{21}$$

Note that we use the isospin convention $\bar{u} = |1/2, -1/2\rangle$ and $\bar{d} = -|1/2, +1/2\rangle$, which induces $D^0 = |1/2, -1/2\rangle$ and $D^+ = -|1/2, +1/2\rangle$.

2.4 Charmonium radiative transitions

As we shall see, the study of the $2P \to 1S, 2S$ charmonium radiative transitions can help to constrain the mixing between the $D^{(*)}\bar{D}^{(*)}$ and $2P$ charmonium degrees of freedom. We write the Lagrangian for these radiative decays, within the dipolar approximation, as follows [48]:

$$\mathcal{L}_\gamma = \delta_n \,\mathrm{Tr}\left(\bar{J}_\mu(2P)\hat{J}(nS)\right)v_\nu F^{\mu\nu} + h.c. \tag{22}$$

$$\begin{aligned}&= \delta_n v^\nu F_{\mu\nu}\Big\{2\eta_c^\dagger h_c^\mu + 2\chi_{2c}^{\mu\sigma}\psi_\sigma^\dagger(nS)\\ &\quad + \frac{2\chi_{0c}}{\sqrt{3}}\psi^{\mu\dagger}(nS) - i\epsilon^\mu_{.\sigma\alpha\beta}\psi^\sigma(nS)v^\alpha\chi_{c1}^\beta\Big\}\end{aligned} \tag{23}$$

where n is the radial quantum number of the 0^{-+} and 1^{--} charmonium states described by the field $\hat{J}(nS)$, $F^{\mu\nu}$ is the electromagnetic tensor and δ_n is a dimensional parameter ($[E^{-1}]$), which also depends on the heavy flavor, at least through the heavy-quark electric charge. The above Lagrangian conserves parity, charge conjugation and it is invariant under HQSS transformations since electric transitions do not change the quark spin. It is straightforward to obtain for the E1 $\chi_{c1}(2P) \to \psi(nS)\gamma$ transition [48]

$$\Gamma\left[\chi_{c1}(2P) \to \psi(nS)\gamma\right] = \frac{\delta_n^2}{3\pi}E_\gamma^3\frac{M_{\psi(nS)}}{m_{\chi_{c1}}} \tag{24}$$

where E_γ is the photon energy. The comparison with the expressions given in Ref. [52] leads to the identification

$$\delta_n = \left(\frac{4\pi\alpha}{3}e_c^2\right)^{\frac{1}{2}}\langle nS|r|2P\rangle,$$

$$\langle nS|r|2P\rangle = \int_0^{+\infty}\mathrm{d}r r^2 R_{nS}(r) r R_{2P}(r), \tag{25}$$

with $e_c = 2/3$, the charm quark electric charge (in proton electric charge units), and the normalization of the radial wave functions given by

$$\int_0^{+\infty}\mathrm{d}r r^2 R_{nL}(r)R_{n'L}(r) = \delta_{nn'}. \tag{26}$$

3 Unitarized isoscalar amplitudes from HQSS LO potentials

In this section, we first give the isoscalar amplitudes obtained by solving the LSE's in coupled channels using as kernels the potentials deduced from the HQSS LO Lagrangians discussed in the previous section. We particularize for the hidden charm molecular and $2P$ quarkonium states, though the extension to the bottom case is straightforward.

For $D\bar{D}^*$, the C-parity states are $[D\bar{D}^*]_\pm = (D\bar{D}^* \mp D^*\bar{D})/\sqrt{2}$, and satisfy $C[D\bar{D}^*]_\pm = \pm[D\bar{D}^*]_\pm$. In our convention, the C-parity of these states is independent of the isospin and it is equal to ± 1. The relevant channels in the different J^{PC} sectors are

$$\begin{aligned}J^{PC} = 0^{++} &: \left\{D\bar{D}, D^*\bar{D}^*, \chi_{c0}(2P)\right\},\\ J^{PC} = 1^{++} &: \left\{\frac{1}{\sqrt{2}}\left(D\bar{D}^* - D^*\bar{D}\right), \chi_{c1}(2P)\right\},\\ J^{PC} = 2^{++} &: \left\{D^*\bar{D}^*, \chi_{c2}(2P)\right\},\\ J^{PC} = 1^{+-} &: \left\{\frac{1}{\sqrt{2}}\left(D^*\bar{D} + D\bar{D}^*\right), D^*\bar{D}^*, h_c(2P)\right\}.\end{aligned} \tag{27}$$

3.1 QM potentials

From the Lagrangians of Eqs. (16) and (20), we obtain Feynman amplitudes, T^{FT}, which in turn are used to define the non-relativistic Quantum Mechanics (QM) potentials, with the convention,

$$\begin{aligned}&V^{\mathrm{QM}}\left[D^{(*)}\bar{D}^{(*)} \to D^{(*)}\bar{D}^{(*)}\right]\\ &= \frac{T^{\mathrm{FT}}\left[D^{(*)}\bar{D}^{(*)} \to D^{(*)}\bar{D}^{(*)}\right]}{\sqrt{2M_{D^{(*)}}2M_{\bar{D}^{(*)}}2M_{D^{(*)}}2M_{\bar{D}^{(*)}}}} = -\frac{\mathcal{L}_{4H}}{4}\end{aligned} \tag{28}$$

$$V_{c\bar{c}}^{\rm QM}\left[\psi_{c\bar{c}}(2P)\to D^{(*)}\bar{D}^{(*)}\right] = \frac{T^{\rm FT}\left[\psi_{c\bar{c}}(2P)\to D^{(*)}\bar{D}^{(*)}\right]}{\sqrt{2\,\mathring{m}_{c\bar{c}}\,2M_{D^{(*)}}2M_{\bar{D}^{(*)}}}} = -\frac{\mathcal{L}_{HHQ\bar{Q}}}{2\sqrt{2}} \tag{29}$$

with $\psi_{c\bar{c}}$, the $\chi_{cJ}(2P)$ or $h_c(2P)$ charmonium state, and $\mathring{m}_{c\bar{c}}$ its common bare mass.[5]

The isoscalar $\left[D^{(*)}\bar{D}^{(*)}\to D^{(*)}\bar{D}^{(*)}\right]$ potentials have been obtained in [33],

$$V^{\rm QM}(1^{++}) = C_{0A} + C_{0B}, \tag{30}$$

$$V^{\rm QM}(0^{++}) = \begin{pmatrix} C_{0A} & \sqrt{3}\,C_{0B} \\ \sqrt{3}\,C_{0B} & C_{0A}-2\,C_{0B}\end{pmatrix}, \tag{31}$$

$$V^{\rm QM}(1^{+-}) = \begin{pmatrix} C_{0A}-C_{0B} & 2\,C_{0B} \\ 2\,C_{0B} & C_{0A}-C_{0B}\end{pmatrix}, \tag{32}$$

$$V^{\rm QM}(2^{++}) = C_{0A} + C_{0B}. \tag{33}$$

Particle coupled-channel[6] effects turn out to be sub-leading at the charm and bottom scales [33,35], and it was also the case for those due to pion exchanges. Hence, in the phenomenological analysis carried out in Refs. [34,36], the off-diagonal elements of the 0^{++} and 1^{+-} potentials were set to zero. However, in the strict heavy-quark limit, where pseudoscalar and vector heavy–light mesons become degenerate, coupled-channel effects need to be considered. In that limit, and after diagonalizing the matrices, there are appear two different eigenvalues $(C_{0a}-3C_{0b})$ and $(C_{0a}+C_{0b})$, associated to the spin $s_l = 0$ and 1 configurations of the light degrees of freedom, respectively. This gives rise to a large number of degenerate molecular states in the heavy-quark limit, as discussed in [45,53].

On the other hand, the $\left[\psi_{c\bar{c}}(2P)\to D^{(*)}\bar{D}^{(*)}\right]$ transition amplitudes are obtained from the Lagrangian of Eq. (20),

$$V_{c\bar{c}}^{\rm QM}(1^{++}) = d \qquad \chi_{c1}(2P)\to[D\bar{D}^*]_+ \tag{34}$$

$$V_{c\bar{c}}^{\rm QM}(0^{++}) = -\frac{\rm d}{2}\begin{pmatrix}\sqrt{3}\\ 1\end{pmatrix} \qquad \begin{pmatrix}\chi_{c0}(2P)\to D\bar{D}\\ \chi_{c0}(2P)\to D^*\bar{D}^*\end{pmatrix} \tag{35}$$

$$V_{c\bar{c}}^{\rm QM}(1^{+-}) = -\frac{\rm d}{\sqrt{2}}\begin{pmatrix}1\\ 1\end{pmatrix} \qquad \begin{pmatrix}h_c(2P)\to[D\bar{D}^*]_-\\ h_c(2P)\to D^*\bar{D}^*\end{pmatrix} \tag{36}$$

$$V_{c\bar{c}}^{\rm QM}(2^{++}) = d \quad \chi_{c2}(2P)\to D^*\bar{D}^*. \tag{37}$$

Due to the use of contact interactions, the LSE shows an ill-defined UV behavior, and it requires a regularization and renormalization procedure. We employ a standard Gaussian regulator (see, e.g. [54])

$$\langle\vec{p}\,';\ D^{(*)}\bar{D}^{(*)}\,|V_\Lambda^{\rm QM}|\vec{p}\,;\ D^{(*)}\bar{D}^{(*)}\rangle = C_{0H}\ f_\Lambda(\vec{p}\,')f_\Lambda(\vec{p}\,) \tag{38}$$

$$\langle\vec{p}\,;\ D^{(*)}\bar{D}^{(*)}\,|V_{c\bar{c};\Lambda}^{\rm QM}|\psi_{c\bar{c}}(2P)\rangle \propto d\ f_\Lambda(\vec{p}\,) \tag{39}$$

with $f_\Lambda(\vec{p}\,) = e^{-\vec{p}^{\,2}/\Lambda^2}$, C_{0H} any of the combinations of isoscalar LECs that appear in Eqs. (30)–(33), and the proportionality constants in Eq. (39) can be read off from Eqs. (34)–(37). We take cutoff values $\Lambda = 0.5$–1 GeV [33,34], where the range is chosen such that Λ will be bigger than the wave number of the states, but at the same time it will be small enough to preserve HQSS and prevent that the theory might become sensitive to the specific details of short-distance dynamics. The dependence of the results on the cutoff, when it varies within this window, provides a rough estimate of the expected size of sub-leading corrections.

3.2 Non-perturbative LSE re-summation

The interplay of quark and meson degrees of freedom in a near-threshold resonance was addressed in Ref. [55]. We study physical states which are mixture of a $c\bar{c}$ bare state and some molecular components. Let us consider a particular J^{PC} sector where there exist $n+1$ coupled channels, and assume that the first n channels are of molecular type,[7] while the last one is $c\bar{c}$. The dynamics of such system of energy E is governed by a generalized $n+1$ dimension t-matrix given by [55] (diagrammatically, the most relevant elements are depicted in Fig. 1),

$$\langle\vec{p}\,'|T(E)|\vec{p}\,\rangle = F_\Lambda(\vec{p}\,')\begin{pmatrix}\left[t_{V^{\rm QM}}+\Gamma_{c\bar{c}}G_{c\bar{c}}\Gamma_{c\bar{c}}^t\right]_{n\times n} & \left[\dfrac{\Gamma_{c\bar{c}}}{1-G_{c\bar{c}}^0\Sigma_{c\bar{c}}}\right]_{n\times 1}\\ \left[\dfrac{\Gamma_{c\bar{c}}^t}{1-G_{c\bar{c}}^0\Sigma_{c\bar{c}}}\right]_{1\times n} & \left[\dfrac{\Sigma_{c\bar{c}}}{1-G_{c\bar{c}}^0\Sigma_{c\bar{c}}}\right]_{1\times 1}\end{pmatrix}F_\Lambda(\vec{p}) \tag{40}$$

where the Gaussian matrix of form factors reads[8]

$$F_\Lambda(\vec{p}\,) = \begin{pmatrix}{\rm Diag}\left[f_\Lambda(\vec{p}\,)\right]_{n\times n} & 0\\ 0 & 1\end{pmatrix}. \tag{41}$$

[5] Note that, here, by bare mass we mean the mass of the charmonium states when the LEC d is set to zero, $d=0$, and thus it is not a physical observable. Coupling to the $D^{(*)}\bar{D}^{(*)}$ meson pairs renormalizes this bare mass, as we will discuss below. Since, in the effective theory, the UV cutoff is finite, the difference between the bare and the physical charmonium masses is a finite renormalization. This shift depends on the UV regulator since the bare mass itself depends on the renormalization scheme. The value of the bare mass, which is thus a free parameter, can either be indirectly fitted to experimental observations, or obtained from schemes that ignore the coupling of charmonium states to the mesons, such as some constituent quark models. In the latter case, the issue certainly would be to set the UV regulator to match the quark model and the EFT approaches.

[6] We do not refer to charge channels, but rather to the $P\bar{P}$ and $P^*\bar{P}^*$ or $P\bar{P}^*$ and $P^*\bar{P}^*$ mixings in the 0^{++} and 1^{+-} sectors, respectively.

[7] We should nevertheless remind the reader here, once more, that molecular coupled-channel effects should not be taken at LO for finite heavy-quark masses, and that those effects appear at next-to-next leading order [33,35].

[8] For on-shell mesons, the form factor depends on the masses of the involved mesons, and hence on the meson channel.

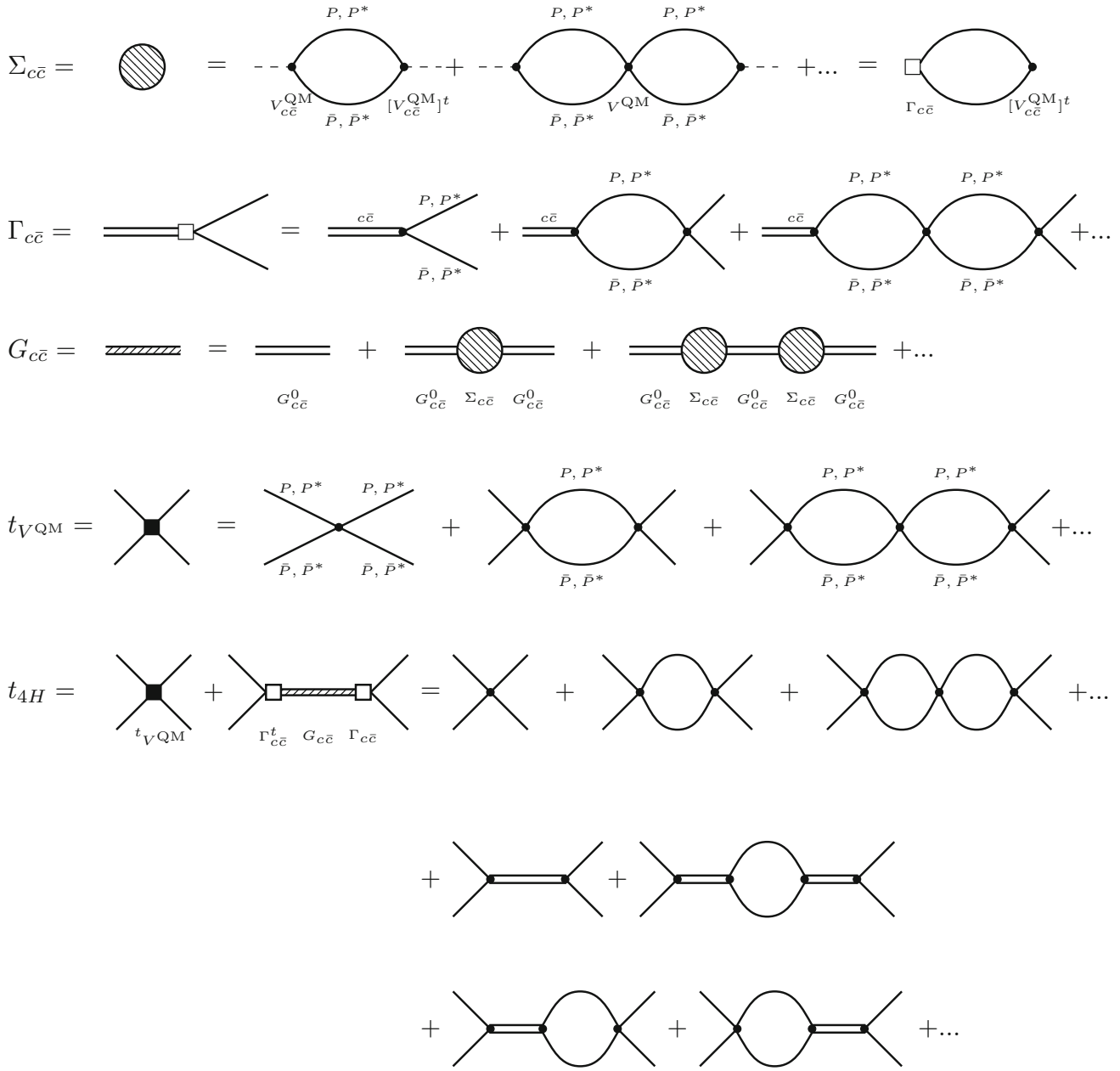

Fig. 1 Diagrammatic representation of different amplitudes: charmonium selfenergy ($\Sigma_{c\bar{c}}$), dressed charmonium propagator ($G_{c\bar{c}}$) and charmonium–$D^{(*)}\bar{D}^{(*)}$ vertex function ($\Gamma_{c\bar{c}}$), "partial" mesonic t-matrix ($t_{V^{\rm QM}}$), and full mesonic t-matrix (t_{4H}) defined in Eq. (50)

On the other hand, the "partial" mesonic t-matrix,[9] $t_{V^{\rm QM}}$ is solution, once the Gaussian form-factor diagonal matrix $f_\Lambda(\vec{p}\,)$ is also considered, of a LSE with kernel $V^{\rm QM}$, and it is given by

$$t_{V^{\rm QM}} = \left(1 - V^{\rm QM} G_{\rm QM}(E)\right)^{-1} V^{\rm QM} \tag{42}$$

with $G_{\rm QM}(E)$, the diagonal meson-loop function, conveniently regularized with the Gaussian form factor. For an arbitrary energy E, its diagonal elements read [42]

$$\begin{aligned} G_{\rm QM}(E) &= \int \frac{{\rm d}^3\vec{q}}{(2\pi)^3} \frac{e^{-2\vec{q}^{\,2}/\Lambda^2}}{E - M_1 - M_2 - \vec{q}^{\,2}/2\mu + i0^+} \\ &= -\frac{\mu\Lambda}{(2\pi)^{3/2}} + \frac{\mu k}{\pi^{3/2}}\phi(\sqrt{2}k/\Lambda) - i\frac{\mu k}{2\pi}e^{-2k^2/\Lambda^2}, \end{aligned} \tag{43}$$

with $\mu^{-1} = M_1^{-1} + M_2^{-1}$, $k^2 = 2\mu(E - M_1 - M_2)$ and $\phi(x)$ the Dawson integral given by

[9] We call it "partial", because it does not incorporate $Q\bar{Q}$ effects on the meson–meson scattering.

$$\phi(x) = e^{-x^2} \int_0^x e^{y^2} \mathrm{d}y. \tag{44}$$

Coming back to the different elements appearing in Eq. (40), the non-relativistic bare $G^0_{c\bar{c}}$ and dressed $G_{c\bar{c}}$ charmonium propagators are given by

$$G^0_{c\bar{c}}(E) = \frac{1}{E - \mathring{m}_{c\bar{c}}}, \quad G_{c\bar{c}}(E) = \frac{1}{E - \mathring{m}_{c\bar{c}} - \Sigma_{c\bar{c}}(E)} \tag{45}$$

where $\Sigma_{c\bar{c}}$ is the charmonium self energy induced by the meson loops,

$$\Sigma_{c\bar{c}}(E) = \left[V^{\mathrm{QM}}_{c\bar{c}}\right]^t G_{\mathrm{QM}}(E) \Gamma_{c\bar{c}}(E) \tag{46}$$

with the dressed vertex function, $\Gamma_{c\bar{c}}$, given by

$$\Gamma_{c\bar{c}}(E) = \left(1 - V^{\mathrm{QM}} G_{\mathrm{QM}}(E)\right)^{-1} V^{\mathrm{QM}}_{c\bar{c}}. \tag{47}$$

Two final remarks. First the t-matrix given in Eq. (40) can also be expressed as a solution of a LSE,

$$\langle \vec{p}\,' | T(E) | \vec{p} \rangle = F_\Lambda(\vec{p}\,') \left(\hat{V}^{-1} - \hat{G}(E)\right)^{-1} F_\Lambda(\vec{p}), \tag{48}$$

$$\hat{V} = \begin{pmatrix} V^{\mathrm{QM}} & V^{\mathrm{QM}}_{c\bar{c}} \\ \left[V^{\mathrm{QM}}_{c\bar{c}}\right]^t & 0 \end{pmatrix},$$

$$\hat{G}(E) = \begin{pmatrix} G_{\mathrm{QM}}(E) & 0 \\ 0 & G^0_{c\bar{c}}(E) \end{pmatrix}, \tag{49}$$

and finally that the full $(n \times n)$-mesonic t-matrix can be obtained as a solution of a LSE equation with an energy dependent effective potential $V_{\mathrm{eff}}(E)$ [55],

$$\begin{aligned} \langle \vec{p}\,' | t_{4H}(E) | \vec{p} \rangle &= f_\Lambda(\vec{p}\,') \left[t_{V^{\mathrm{QM}}} + \Gamma_{c\bar{c}} G_{c\bar{c}} \Gamma^t_{c\bar{c}}\right] f_\Lambda(\vec{p}) \\ &= \left(f^{-1}_\Lambda(\vec{p}) \left[-G_{\mathrm{QM}}(E) + V^{-1}_{\mathrm{eff}}(E)\right] f^{-1}_\Lambda(\vec{p}\,')\right)^{-1}, \end{aligned} \tag{50}$$

$$\begin{aligned} V_{\mathrm{eff}}(E) &= V^{\mathrm{QM}} + V^{\mathrm{QM}}_{c\bar{c}} G^0_{c\bar{c}}(E) \left[V^{\mathrm{QM}}_{c\bar{c}}\right]^t \\ &= V^{\mathrm{QM}} + \frac{V^{\mathrm{QM}}_{c\bar{c}} \left[V^{\mathrm{QM}}_{c\bar{c}}\right]^t}{E - \mathring{m}_{c\bar{c}}}. \end{aligned} \tag{51}$$

In the strict heavy-quark limit, where the full coupled-channel effects should be considered, the effective matrix potential $V_{\mathrm{eff}}(E)$ gives rise to two different eigenvalues, $(C_{0a} - 3C_{0b})$ and $(C_{0a} + C_{0b}) + d^2/(E - \mathring{m}_{c\bar{c}})$. Thus, as compared to those deduced from V^{QM}, the interaction in the $s_l = 0$ configuration has not been modified, while the $s_l = 1$ one is affected by the coupling to the quarkonium states. The extra interaction becomes repulsive or attractive depending on whether the energy E is above or below the bare charmonium mass, $\mathring{m}_{c\bar{c}}$. Nevertheless we should stress, as mentioned above, that in the present scheme $\mathring{m}_{c\bar{c}}$ is a free parameter and it is not an observable, which gets dressed by the $D^{(*)}$-meson loops and gives rise to the physical mass of the charmonium states (see for instance the discussion below Table 1, Fig. 2 for the 1^{++} sector).

4 Poles of the unitarized amplitudes and the compositeness condition

4.1 Bound, resonant states and couplings

The dynamically generated meson states appear as poles of the scattering amplitudes on the complex energy E-plane. The poles of the scattering amplitude on the first Riemann sheet (FRS) that appear on the real axis below threshold are interpreted as bound states. The poles that are found on the second Riemann sheet (SRS) below the real axis and above threshold are identified with resonances. The mass and the width of the state can be found from the position of the pole on the complex energy plane. Close to the pole, the scattering amplitude behaves as

$$T_{ij} \sim \frac{g_i g_j}{E - E_R}. \tag{52}$$

The mass M_R and width Γ_R of the state result from $E_R = M_R - i\Gamma_R/2$, while g_j (complex in general) is the coupling of the state to the j-channel.

The meson-loop function was given in Eq. (43). Note that the wave number k is a multivalued function of E, with a branch point at threshold ($E = M_1 + M_2$). The principal argument of $(E - M_1 - M_2)$ should be taken in the range $[0, 2\pi[$. Note that this amounts to choosing the branch cut of the square root function defining k, to lie on the positive real line. The function $k\phi(\sqrt{2}k/\Lambda)$ does not present any discontinuity for real E above threshold, and $G_{\mathrm{QM}}(E)$ becomes a multivalued function because of the ik term. Indeed, $G_{\mathrm{QM}}(E)$ has two Riemann sheets. In the first one, $0 \leqslant \mathrm{Arg}(E - M_1 - M_2) < 2\pi$, we find a discontinuity $G^I_{\mathrm{QM}}(E + i\epsilon) - G^I_{\mathrm{QM}}(E - i\epsilon) = 2i\,\mathrm{Im}G^I_{\mathrm{QM}}(E + i\epsilon)$ for $E > (M_1 + M_2)$. In the second Riemann sheet, $2\pi \leqslant \mathrm{Arg}(E - M_1 - M_2) < 4\pi$, we trivially find $G^{II}_{\mathrm{QM}}(E - i\epsilon) = G^I_{\mathrm{QM}}(E + i\epsilon)$, for real energies and above threshold.

4.2 Components of the states and the compositeness condition

It is difficult to pin down the exact nature of a hadronic state since wave functions are not observables themselves. The claims regarding the largest Fock components in a wave function are often model dependent. The compositeness condition, first proposed by Weinberg to explain the deuteron as a neutron–proton bound state [56,57], has been advocated as a model independent way to determine the relevance of hadron-hadron components in a molecular state. However, this is strictly only valid for bound states. For resonances, it

Table 1 Properties of the 1^{++} hidden charm poles as a function of d. We solve Eq. (61) with $\Lambda = 1.0$ GeV and for each value of d, C_{0X} is determined by Eq. (71). The position of the $X(3872)$ is fixed at $M_X = 3871.69$ MeV in the FRS. The $\chi_{c1}(2P)$ pole is located in the SRS. Finally, $d^{\,\mathrm{crit}}(\Lambda = 1\,\mathrm{GeV}) = \sqrt{\frac{M_X - \mathring{m}_{\chi_{c1}}}{G^I_{\mathrm{QM}}(M_X)}} = 0.370\ \mathrm{fm}^{1/2}$

d [fm$^{1/2}$]	C_{0X} [fm^2]	$g^{X(3872)}_{D\bar{D}^*}$ [GeV$^{-1/2}$]	$\tilde{X}_{X(3872)}$	$(m_{\chi_{c1}}, \Gamma_{\chi_{c1}})$ [MeV]	$g^{\chi_{c1}}_{D\bar{D}^*}$ [GeV$^{-1/2}$]	$\lvert\tilde{X}_{\chi_{c1}}\rvert$	$\tilde{Z}_{\chi_{c1}}$
0.	−0.789	0.90	1	(3906.0,0)	0.	0.	1.
0.05	−0.774	0.89	0.98	(3906.6, 1.9)	$0.01 + 0.16\,i$	0.02	$0.99 + 0.01\,i$
0.1	−0.731	0.87	0.92	(3908.2, 7.9)	$0.03 + 0.31\,i$	0.06	$0.96 + 0.05\,i$
0.15	−0.659	0.83	0.84	(3910.5, 19.2)	$0.07 + 0.44\,i$	0.14	$0.92 + 0.11\,i$
0.20	−0.559	0.78	0.75	(3912.4, 37.8)	$0.14 + 0.56\,i$	0.23	$0.87 + 0.19\,i$
0.25	−0.429	0.73	0.66	(3912.0, 67.0)	$0.24 + 0.65\,i$	0.36	$0.82 + 0.31\,i$
0.30	−0.271	0.68	0.57	(3903.9, 112.8)	$0.38 + 0.73\,i$	0.55	$0.77 + 0.50\,i$
0.35	−0.084	0.63	0.49	(3864.5, 185.2)	$0.63 + 0.85\,i$	>1	$0.70 + 1.01\,i$
$d^{\,\mathrm{crit}}$	0.000	0.61	0.47	(3798.3, 209.4)	$0.93 + 1.09\,i$	>1	$0.53 + 2.12\,i$
0.375	0.020	0.61	0.46	(3754.4, 186.4)	$1.21 + 1.37\,i$	>1	$0.29 + 3.66\,i$
0.3775	0.031	0.61	0.46	(3701.6, 93.5)	$2.19 + 2.39\,i$	>1	$-0.44 + 12.27\,i$
0.40	0.132	0.59	0.43	(3827.1, 0) at SRS	0.96	$\tilde{X}_{\chi_{c1}} < 0$	2.07
0.45	0.376	0.55	0.37	(3850.9,0) at SRS	0.63	$\tilde{X}_{\chi_{c1}} < 0$	1.52
0.5	0.649	0.51	0.32	(3858.4,0) at SRS	0.51	$\tilde{X}_{\chi_{c1}} < 0$	1.36
1.0	4.963	0.29	0.11	(3869.7, 0) at SRS	0.21	$\tilde{X}_{\chi_{c1}} < 0$	1.08
2.0	22.217	0.15	0.03	(3871.3, 0) at SRS	0.10	$\tilde{X}_{\chi_{c1}} < 0$	1.02
$d \gg d^{\,\mathrm{crit}}$	$\sim \frac{d^2}{\mathring{m}_{\chi_{c1}} - M_X}$	$\mathcal{O}(1/d)$	$\mathcal{O}(1/d^2)$	$(M_X - \mathcal{O}(\frac{1}{d^2}), 0)$ at SRS	$\mathcal{O}(1/d)$	$\tilde{X}_{\chi_{c1}} = -\mathcal{O}(\frac{1}{d^2})$	$1 + \mathcal{O}(\frac{1}{d^2})$

involves complex numbers and, therefore, a strict probabilistic interpretation is lost. The probabilistic interpretation of the compositeness condition has its origin in the sum rule [58–60]

$$-1 = \sum_{ij} g_i g_j \left(\delta_{ij} \left[\frac{\partial G_i^{II}(E)}{\partial E} \right]_{E=E_R} + \left[G_i^{II}(E) \frac{\partial V_{ij}(E)}{\partial E} G_j^{II}(E) \right]_{E=E_R} \right), \tag{53}$$

which is satisfied by the residues of a pole, located in the fourth quadrant of the SRS, of a t-matrix solution of a coupled–channel LSE,

$$T^{-1} = -G + V^{-1}. \tag{54}$$

The above sum rule[10] is also satisfied in the case of bound states (poles located in the real axis of the FRS below the lowest of the thresholds) replacing $G^{II} \leftrightarrow G^I$. From Eq. (53), one might think that a possible definition of the weight of a hadron-hadron component in a composite particle could be

$$X_i = \mathrm{Re}\tilde{X}_i = \mathrm{Re}\left(-g_i^2 \left[\frac{\partial G_i^{II}(E)}{\partial E} \right]_{E=E_R} \right). \tag{55}$$

As follows from the analysis in [17,61], for bound states, the quantity $\tilde{X}_i$ is real and it is related to the probability of finding the state in the channel i. For resonances, $\tilde{X}_i$ is still related to the squared wave function of the channel i, in a phase prescription that automatically renders the wave function real for bound states, and so it can be used as a measure of the weight of that meson-baryon channel in the composition of the resonant state [59,61]. The deviation of the sum of X_i from unity is related to the energy dependence of the S-wave potential,

$$\sum_i X_i = 1 - Z, \tag{56}$$

where

$$Z = \mathrm{Re}\tilde{Z} = \mathrm{Re}\left(-\sum_{ij} \left[g_i G_i^{II}(E) \frac{\partial V_{ij}(E)}{\partial E} G_j^{II}(E) g_j \right]_{E=E_R} \right). \tag{57}$$

Note that Eq. (53) guaranties that the imaginary parts of $\sum_i \tilde{X}_i$ and $\tilde{Z}$ must cancel. The quantity $\tilde{Z}$, though complex in general, is defined even for resonances, since it is related

[10] We should note that Eq. (53) is not the original Weinberg condition [56,57], though it is undoubtedly inspired by the findings of this work.

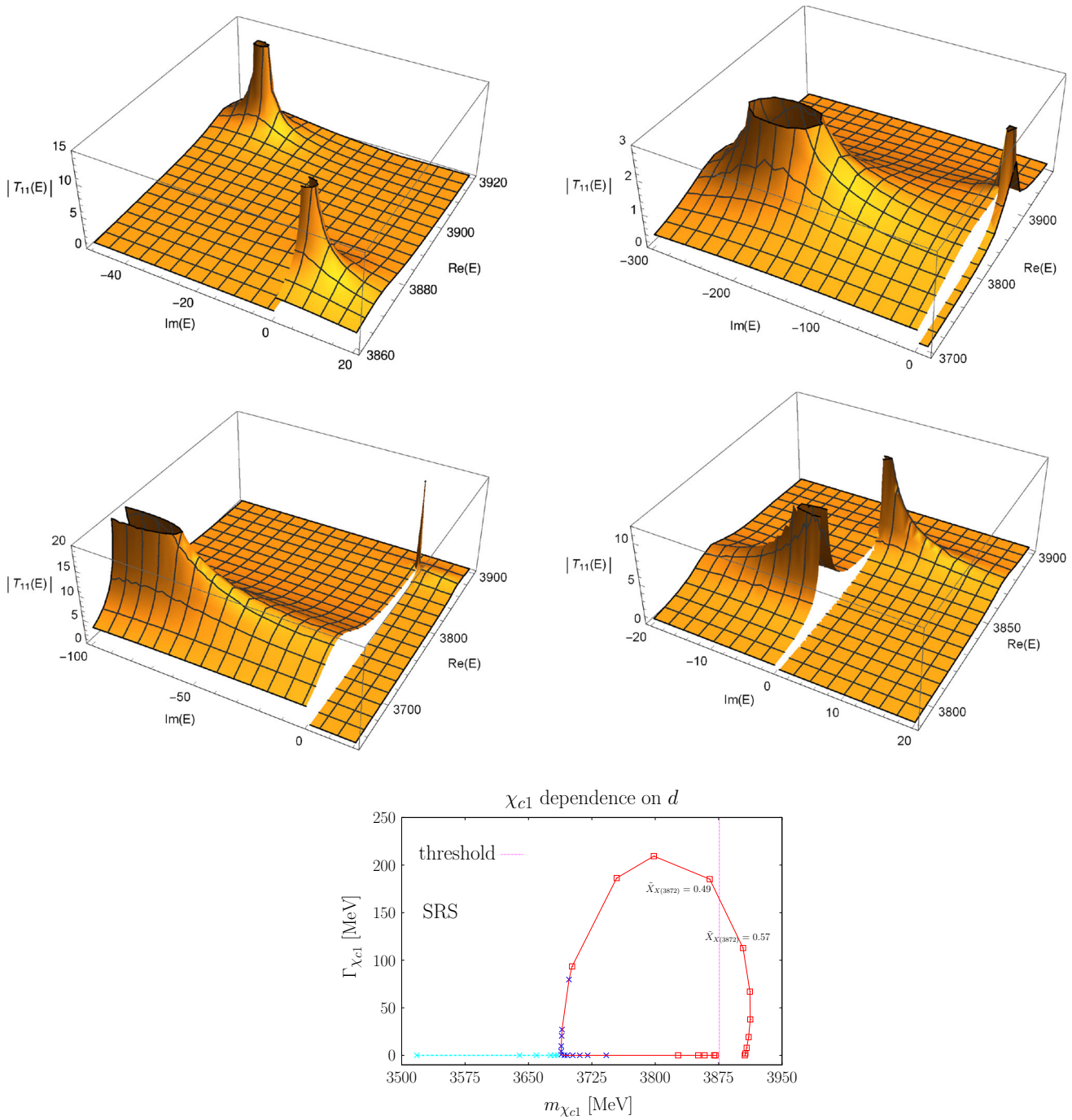

Fig. 2 Hidden charm $J^{PC} = 1^{++}$ sector. *Top* and *middle panels* FRS ($\mathrm{Im}(E) > 0$) and SRS ($\mathrm{Im}(E) < 0$) of $|T_{11}(E)|$ [fm^2] (Eq. (59)) as a function of the complex energy E [MeV], for $d = 0.20$, d^{crit}, 0.3775 and 0.40 fm$^{1/2}$. Note that, since the T-matrix is shown for only half of the SRS (and also the FRS), the pole in the SRS conjugate to the pole shown in the figures is not visible. *Bottom panel* dependence of the $\chi_{c1}(2P)$ mass and width on d. Squares stand for the results of Table 1 at different values of d, while the crosses illustrate the highly non-linear behavior that appears when d takes values in the interval [0.3776, 0.3785] fm$^{1/2}$. In the latter case, when the pole reaches the real axis, we find two poles, which start separating from each other and move apart from the "meeting point" (intersection with the real axis). Note that no information as regards the pole that departs from threshold (*cyan crosses*) is given in Table 1. The curve is smooth except at the point where the pole hits the real axis on the SRS, however, it looks like a broken line because the points are connected by straight segments. All calculations have been carried out with an UV cutoff $\Lambda = 1$ GeV

to the field renormalization constant [62] that is obtained by requiring that the residue of the renormalized two point function will be one. However, its probabilistic interpretation is not straightforward. Thus, though $\tilde{X}_i$ can be interpreted as a probability of finding a two-body component in a bound state, this interpretation, strictly speaking, cannot be made in the case of a resonance. Nevertheless, because it represents the contribution of the channel wave function to the total normalization, the compositeness $\tilde{X}_i$ will have an important piece of information on the structure of the resonance. Moreover, in Ref. [63], it was claimed that one can formulate a meaningful compositeness relation with only positive coefficients thanks to a suitable transformation of the S matrix. This in practice amounts to take the absolute value of $\tilde{X}_i$ to quantify the probability of finding a specific component in the wave function of a hadron. Notice, however, that the recipe advocated in Ref. [63] is not applicable to all types of poles. In particular the arguments of this reference exclude the case of virtual states or resonant signals which are an admixture between a pole and an enhanced cusp effect by the pole itself. More specifically, the probabilistic interpretation given in [63] to $|\tilde{X}_i|$ is only valid when $\mathrm{Re}(E_R) > M_{i,\mathrm{th}}$, with $M_{i,\mathrm{th}}$ the corresponding threshold of the channel i.

For the present study, since the V^{QM} and $V_{c\bar{c}}$ potentials do not depend on the energy, Eqs. (48) and (49) should guarantee that the residues of the poles of the on-shell $\langle \vec{p}\,' | T(E) | \vec{p}\,\rangle$ will fulfill

$$-\sum_i g_i^2 \left(\frac{\partial \left[\hat{G}_i(E)/F_{\Lambda\, i}^2 \right]}{\partial E} \right)_{E=E_R} = 1 \tag{58}$$

where the loop function should be computed in the FRS or SRS as appropriate. Note that the above equation is not strictly correct, and there exist minor corrections induced by the mild energy dependence induced in the potentials inherited from the form-factor matrix $F_\Lambda(E)$. We will make use of the above sum rule to address the molecular meson–meson content of the various poles obtained in the next subsection.

On the other hand, if we restrict ourselves to the full mesonic t-matrix defined in Eq. (50), we will face a situation like that described in Eqs. (56) and (57). This is because, t_{4H} is defined by means of an energy–dependent effective potential result of integrating out the quarkonium degrees of freedom. In the latter context, X_i and Z will be related to the weights of the two-body molecular and the integrated out elementary (quarkonium) components, respectively.

5 Quarkonium and the 1^{++} and 2^{++} meson molecules

HQSS predicts that in the heavy-quark limit, the interaction in both the 1^{++} and 2^{++} sectors should be identical. Moreover, the dynamics in these sectors is governed by the $s_l = 1$ configuration of the light degrees of freedom, which is precisely that affected by the coupling between quarkonium and meson–antimeson states. At the charm scale, we expect some HQSS breaking effects due to the $D - D^*$, and the bare $\chi_{c1}(2P) - \chi_{c2}(2P)$ mass differences.

As mentioned in the introduction, assuming the $X(3872)$ to be a $D\bar{D}^*$ molecule, the existence of a $X_2[J^{PC} = 2^{++}]$ S-wave $D^*\bar{D}^*$ bound state was predicted in Refs. [33,34], with a binding energy similar to that of the $X(3872)$. The X_2 is not affected by particle coupled-channel effects and its mass only varies mildly, by about 2–3 MeV, when corrections from the one pion exchange potential are taken into account [33]. This prediction is subject to some uncertainties because of the approximate nature of HQSS. Hence, the state might move slightly up above the $D^*\bar{D}^*$ threshold and become virtual or might descend to a lower mass region [36]. Be that as it may, one could be quite confident about the existence of a molecular state with these quantum numbers close to the $D^*\bar{D}^*$ threshold. However, the state has not been observed yet.

Within the EFT approach of Refs. [33,34], it is assumed that the four-meson contact operator absorbs all the details of the short-range dynamics present in the system, such as light vector meson exchanges between the charmed mesons, or other Fock components in the $X(3872)$ and $X_2(4012)$ wave functions. However, the effects due to the presence of the $2P$ quarkonium states could be sizable, in particular in the 1^{++} sector, because one expects the corresponding $c\bar{c}$ state to lie close to the $X(3872)$ [52]. The experimental $\chi_{c2}(2P)$ mass, $m_{\chi_{c2}}^{\mathrm{exp}} = 3927.2 \pm 2.6$ MeV [6], is significantly lower than the $D^*\bar{D}^*$ threshold, and hence it looks reasonable to expect a limited influence of the charmonium level in the dynamics of a loosely 2^{++} state located in the vicinity of the $D^*\bar{D}^*$ threshold. However, one should bear in mind that if the $\chi_{c1}(2P)$ is above the $D\bar{D}^*$ threshold, but relatively close to it, the presence of the charmonium state would provide an effective attraction that will contribute to binding the $X(3872)$, but it will not appear in the 2^{++} sector.[11] Because we are dealing with very weakly bound states, it might well occur that these effects need to be explicitly considered and they cannot be just accounted for in short-distance LECs. This is what we want to qualitatively illustrate in this section. To that end, and for simplicity, we work in the isospin-symmetric limit as done in Refs. [33,36] and in the LQCD study of Ref. [38], and use the averaged masses of the heavy mesons, which are $M_D = 1867.24$ MeV, $M_{D^*} = 2008.63$ MeV, while we take the central value of the particle data group (PDG) averaged

[11] Indeed, the $\chi_{c2}(2P)$ would provide an effective repulsion in this case, since it is placed below the $D^*\bar{D}^*$ threshold. Nevertheless, as commented before, the strength of such interaction would presumably be small since the $\chi_{c2}(2P)$ mass is significantly (90 MeV) lighter than the two body threshold.

mass for the $X(3872)$, $M_X = 3871.69 \pm 0.17\,\text{MeV}$ [6]. We are aware of the importance of the isospin breaking effects in the dynamics of this resonance, specially in its strong decays, and we refer the reader to Refs. [34,64] for a comprehensive discussion. Taking into account such effects might obscure the approach, which in this exploratory study needs to be qualitative, because the existing uncertainties in the masses of the bare $\chi_{c1}(2P)$ and $\chi_{c2}(2P)$ states and in the value of the LEC that mixes meson-molecular and quarkonium components.

In the isoscalar 1^{++} and 2^{++} sectors (from now on, we will be always referring to isoscalar sectors, but for the sake of brevity, we will not explicitly mention it), the on-shell t-matrix of Eq. (40) reads (we particularize it for the hidden charm sectors, but its extension to the bottom ones is straightforward)

$$T(E) = \frac{\Sigma_{c\bar{c}}}{1 - G^0_{c\bar{c}}\Sigma_{c\bar{c}}} \times \begin{pmatrix} f_\Lambda^2(E)\left[(d\,G_{\rm QM})^{-2} - \dfrac{1 - G^0_{c\bar{c}}\Sigma_{c\bar{c}}}{G_{\rm QM}\Sigma_{c\bar{c}}}\right] & f_\Lambda(E)\,(d\,G_{\rm QM})^{-1} \\ f_\Lambda(E)\,(d\,G_{\rm QM})^{-1} & 1 \end{pmatrix} \tag{59}$$

with the on-shell form factor, $f_\Lambda(E) = \exp\{-2\mu(E - M_1 - M_2)/\Lambda^2\}$, and the quarkonium self energy given by

$$\Sigma_{c\bar{c}}(E) = \frac{d^2\,G_{\rm QM}(E)}{1 - C_{0X}\,G_{\rm QM}(E)} \tag{60}$$

where $C_{0X} = C_{0A} + C_{0B}$. The only differences between the 1^{++} and 2^{++} sectors are due to the meson and bare charmonium masses, which appear in the loop function, $G_{\rm QM}(E)$, $c\bar{c}$ bare propagator ($G^0_{c\bar{c}}$) and Gaussian form factors. We use ($M_1 = M_D$, $M_2 = M_{D^*}$, $\mathring{m}_{\chi_{c1}}$) and ($M_1 = M_2 = M_{D^*}$, $\mathring{m}_{\chi_{c2}}$) for the 1^{++} and 2^{++} sectors, respectively. As long as $d \neq 0$, poles[12] of $T(E)$ correspond to zeros of the inverse of the dressed propagator

$$G_{c\bar{c}}(E_R)^{-1} = 0 \leftrightarrow 1 - G^0_{c\bar{c}}(E_R)\Sigma_{c\bar{c}}(E_R) = 0, \quad E_R = M_R - i\Gamma_R/2 \tag{61}$$

in either the FRS (in that case $\Gamma_R \to 0^-$) or the SRS as appropriate. In the vicinity of the pole, we have in the corresponding Riemann sheet

$$\frac{\Sigma_{c\bar{c}}(E)}{1 - G^0_{c\bar{c}}(E)\Sigma_{c\bar{c}}(E)} \sim \frac{1}{E - E_R}\,\frac{\Sigma^2_{c\bar{c}}(E_R)}{1 - \Sigma'_{c\bar{c}}(E_R)}, \quad \Sigma'_{c\bar{c}}(E_R) = \left.\frac{d\Sigma_{c\bar{c}}(E)}{dE}\right|_{E=E_R}, \tag{62}$$

from which it follows that the couplings to the meson–antimeson and bare charmonium states are

$$g_1^2 = \frac{\Sigma^2_{c\bar{c}}(E_R)}{1 - \Sigma'_{c\bar{c}}(E_R)}\,\frac{f_\Lambda^2}{d^2\left[G_{\rm QM}(E_R)\right]^2} = \frac{\Sigma'_{c\bar{c}}(E_R)}{1 - \Sigma'_{c\bar{c}}(E_R)}\,\frac{f_\Lambda^2}{G'_{\rm QM}(E_R)}, \tag{63}$$

$$g_2^2 = \frac{\Sigma^2_{c\bar{c}}(E_R)}{1 - \Sigma'_{c\bar{c}}(E_R)} = \frac{(E_R - \mathring{m}_{c\bar{c}})^2}{1 - \Sigma'_{c\bar{c}}(E_R)} = -\frac{1}{1 - \Sigma'_{c\bar{c}}(E_R)}\,\frac{1}{G^{0\prime}_{c\bar{c}}(E_R)}, \tag{64}$$

where

$$G'_{\rm QM}(E_R) = \left.\frac{dG_{\rm QM}(E)}{dE}\right|_{E=E_R}, \quad G^{0\prime}_{c\bar{c}}(E_R) = \left.\frac{dG^0_{c\bar{c}}(E)}{dE}\right|_{E=E_R}. \tag{65}$$

On the other hand, Eq. (58) is satisfied, and it leads to

$$g_1^2\left(\frac{d\left[G_{\rm QM}(E)/f_\Lambda^2\right]}{dE}\right)_{E=E_R} + g_2^2\left(\frac{d\,G^0_{c\bar{c}}(E)}{dE}\right)_{E=E_R} = \frac{\Sigma'_{c\bar{c}}(E_R)}{1 - \Sigma'_{c\bar{c}}(E_R)} - \frac{1}{1 - \Sigma'_{c\bar{c}}(E_R)} + \cdots = -1 + \cdots \tag{66}$$

where the corrections neglected above are of order $\mathcal{O}\left(\frac{f'_\Lambda(E_R)/f_\Lambda(E_R)}{G'_{\rm QM}(E_R)/G_{\rm QM}(E_R)}\right)$. These corrections, which for $E_R = M_X$ are of the order of 5 %, appear because the form factor induces a mild energy dependence in the $4H$ potential. As expected from the discussion of Eq. (57), we find

$$g_1^2\left(\frac{d\left[V_{\rm eff}^{-1}(E)/f_\Lambda^2\right]}{dE}\right)_{E=E_R} = \frac{1}{1 - \Sigma'_{c\bar{c}}(E_R)} + \mathcal{O}\left(\frac{f'_\Lambda(E_R)/f_\Lambda(E_R)}{V^{-1\prime}_{\rm eff}(E_R)/V^{-1}_{\rm eff}(E_R)}\right). \tag{67}$$

Thus, in the 1^{++} and 2^{++} sectors we define the molecular ($\tilde{X}$) and charmonium ($\tilde{Z}$) probabilities, weights in general, of the pole placed at $E_R = M_R - i\Gamma_R/2$ as

$$\tilde{X} = -\frac{\Sigma'_{c\bar{c}}(E_R)}{1 - \Sigma'_{c\bar{c}}(E_R)}, \quad \tilde{Z} = \frac{1}{1 - \Sigma'_{c\bar{c}}(E_R)}, \tag{68}$$

[12] Note that when $d \to 0$, the t-matrix reduces to

$$\lim_{d\to 0} T(E) = \begin{pmatrix} f_\Lambda^2\,\frac{C_{0X}}{1 - C_{0X}G_{\rm QM}} & 0 \\ 0 & 0 \end{pmatrix}.$$

and $\Sigma'_{c\bar{c}}(E_R)$ is given by

$$\Sigma'_{c\bar{c}}(E_R) = \frac{G'_{\rm QM}(E_R)(E_R - \mathring{m}_{c\bar{c}})^2}{d^2 G^2_{\rm QM}(E_R)}, \tag{69}$$

from which we trivially find that the resonance couples to the charmonium state through the meson loops,

$$g_2 = d\,\frac{g_1}{f_\Lambda}\,G_{\rm QM}(E_R). \tag{70}$$

Besides, we can fix C_{0X} in the presence of the mixing LEC d, by requiring the $X(3872)$ resonance to be a 1^{++} bound state located in the FRS below the $D\bar{D}^*$ threshold. This leads to

$$C_{0X} = \frac{1}{G^I_{\rm QM}(M_X)} - \frac{d^2}{M_X - \mathring{m}_{\chi_{c1}}}, \tag{71}$$

which leaves us with only three undetermined parameters, d, $\mathring{m}_{\chi_{c1}}$, and $\mathring{m}_{\chi_{c2}}$, for the present simultaneous analysis of the 1^{++} and 2^{++} sectors, including mixing with charmonium states.

5.1 Numerical results: $X(3872)$ and $\chi_{c1}(2P)$

One of the greatest uncertainties of the present approach is the mass of the bare $\chi_{c1}(2P)$ state. This state has not been identified yet, while most recent constituent quark models predict masses for the $\chi_{c1}(2P)$ ranging from around 3947.4 MeV [43,65] to 3906 MeV [66], including the value of 3925 MeV obtained in the classic work of Barnes et al. [52]. However, all these models overestimate the measured mass of the $\chi_{c2}(2P)$ for which these works report 3969, 3949, and 3975 MeV, respectively. (We expect small effects from the $D^*\bar{D}^*$ loops, as discussed above.) In this exploratory study, we take

$$\mathring{m}_{\chi_{c1}} = 3906\,\text{MeV} \tag{72}$$

from Ref. [66], since this work provides the closest prediction to the experimental mass of the $\chi_{c2}(2P)$ state. Nevertheless, we should remind the reader here that the bare mass depends on the UV regulator, since it is not a physical observable. Furthermore, and as we already mentioned, there exists the major problem of choosing the appropriate scale to match the constituent quark model and the EFT. At this point, we have adopted a pragmatic view, and thus predictions obtained with two different UV cutoffs, spanning a physically motivated range of values, will be presented. The expectation is that the UV regulator dependence will be absorbed into the LECs and thus predictions for observables at the end could become at most mildly regulator dependent.

5.1.1 *Influence of the d LEC on the properties of the* 1^{++} *hidden charm poles*

In Table 1, we show the properties of the poles found in the 1^{++} hidden charm sector as a function of the mixing LEC d. We solve Eq. (61) with an UV cutoff of $\Lambda = 1$ GeV, the qualitative pattern of the results is similar for 500 MeV, though some quantitative differences appear, as can be seen in Table 6 of the appendix. Note that $C_{0X} = C_{0X}(\Lambda)$, and this dependence on the UV regulator should cancel that of the meson-loop propagator $G_{\rm QM}$ (Eq. (43)), such that observables (resonances masses, widths, meson–meson scattering lengths, etc.) become independent of the UV regulator (see discussion in [33]), up to higher order terms. This is accomplished by definition for the $X(3872)$ mass, but, however, there exists some residual UV-cutoff dependence in its coupling to the $D\bar{D}^*$ meson pair (see Tables 1, 6). The mixing parameter d also depends on Λ. Thus, when we say that both, 1 and 0.5 GeV, UV cutoffs lead to a qualitative similar dependence on d, we mean this, not for specific values of d, but for results obtained for both cutoffs with values of d which give rise to similar meson-molecular probabilities for the $X(3872)$ resonance ($\tilde{X}_{X(3872)}$).

In principle, we expect to find two poles,[13] which will be identified as the $X(3872)$ and the physical $\chi_{c1}(2P)$ states. Because of the election of C_{0X} in Eq. (71), the position of the $X(3872)$ is fixed at $M_X = 3871.69$ MeV, while its molecular probability ($\tilde{X}_{X(3872)}$) and the $D\bar{D}^*$ coupling decrease with d. This is because C_{0X} absorbs all dependence on d, since $G^I_{\rm QM}(M_X)$ accounts only for the unitary logarithms and it is independent of this LEC within the UV-cutoff scheme adopted here, which guaranties that $\Sigma'_{c\bar{c}}(E_R)$ in Eq. (69) scales as $1/d^2$.

On the other hand, the mass and the width of the $\chi_{c1}(2P)$ dressed state strongly depend on d. For moderate values of this LEC, up to $\tilde{X}_{X(3872)} > 0.57$, the pole stays in the SRS above threshold with its width increasing rapidly (f.i. top left panel of Fig. 2). There is a point in the vicinity of $d^{\rm crit}$, value of the LEC for which C_{0X} is zero, where the $\chi_{c1}(2P)$ pole becomes below threshold and quite wide. Since SRS and FRS are disconnected below threshold, such virtual state becomes irrelevant (f.i. top right and middle left panels of Fig. 2). When $C_{0X} = 0$, the pole position equation reduces to

$$E_R = \mathring{m}_{\chi_{c1}} + \left(M_X - \mathring{m}_{\chi_{c1}}\right)\frac{G_{\rm QM}(E_R)}{G^I_{\rm QM}(M_X)},$$
$$E_R = M_R - i\Gamma_R/2, \tag{73}$$

[13] In the SRS, the poles appear as conjugate pairs [67] if they are not on the real axis. We count these as single poles since they correspond to the same resonance.

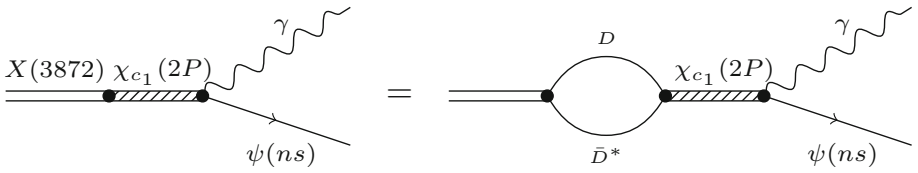

Fig. 3 Decay mechanism for the transition $X(3872) \to \psi(nS)$ through an intermediate charmonium $\chi_{c1}(2P)$ state. The identity between the two diagrams follows from the relation between couplings in Eq. (70)

which, besides $E_R = M_X$ in the FRS, has solutions in the SRS, but below threshold. When C_{0X} becomes positive (repulsive), the pole moves fast to the real axis because there exist solutions only when $M_R < \mathring{m}_{\chi_{c1}}$ and

$$\frac{C_{0X}}{d^2}\left(\left(M_R - \mathring{m}_{\chi_{c1}}\right)^2 + \frac{\Gamma_R^2}{4}\right) \leq |M_R - \mathring{m}_{\chi_{c1}}| \tag{74}$$

as deduced from the imaginary part of Eq. (61), taking into account that $\mathrm{Re}\left(G_{\mathrm{QM}}^{II}\right) < 0$ in this region. The intersection with the SRS real axis occurs for $d \sim 0.377823\,\mathrm{fm}^{1/2}$ that gives rise to a pole at $E_R = M_{0R} - i0$, with $M_{0R} \sim 3688.67\,\mathrm{MeV}$. It turns out that in this intersection $\Sigma'_{c\bar{c}}(M_{0R} - i0) = 1$ leading to singularities in $\tilde{X}_{\chi_{c1}}$ and $\tilde{Z}_{\chi_{c1}}$, and provoking that not only the inverse of the dressed propagator has a zero in this intersection $\left[G_{c\bar{c}}(M_{0R} - i0)^{-1} = G^0_{c\bar{c}}(M_{0R})^{-1} - \Sigma_{c\bar{c}}(M_{0R} - i0) = 0\right]$, but also its first derivative, ie. $dG^{-1}_{c\bar{c}}(E)/dE|_{E=M_{0R}-i0} = 0$. Indeed, it is a double pole (see Eq. (62)) since, as mentioned above, the poles appear as conjugate pairs, which obviously coincide in the real axis producing a kink. Once the poles collide on the real axis, they do not need to remain as a conjugate pair. Indeed, as one pole approaches the threshold, with $\Sigma'_{c\bar{c}}$ decreasing and departing from 1, a second pole moves away from the threshold, with now $\Sigma'_{c\bar{c}}$ taking values above 1. (This behavior coincides with that discussed in Fig. 3 of Ref. [67].) When $d \sim 0.37854\,\mathrm{fm}^{1/2}$, this second pole leaves the real axis forming another conjugate pair, with a mass of around 3470 MeV quite far from threshold. The trajectories of this new conjugate pair as d increases are either below threshold, or above threshold, but in the latter case very deep in the complex plane[14] (widths of around 1 GeV). Hence, these poles will not have any observable consequences, and for simplicity, we will simply ignore them, and we have neither included their details in Table 1. Actually in the following, we will always refer to the pole that moves along the real axis toward threshold. Once, this pole has reached the SRS real axis (f.i. middle right plot of Fig. 2), its position, M_R, is solution (below threshold) of

$$\left(M_R - \mathring{m}_{\chi_{c1}}\right)\left(\frac{1}{G^{II}_{\mathrm{QM}}(M_R)} - \frac{1}{G^{I}_{\mathrm{QM}}(M_X)}\right) = d^2\left(1 - \frac{M_R - \mathring{m}_{\chi_{c1}}}{M_X - \mathring{m}_{\chi_{c1}}}\right), \tag{75}$$

which differs from M_X because $G^I_{\mathrm{QM}}(M_X) \neq G^{II}_{\mathrm{QM}}(M_X)$. This non-trivial d-behavior is illustrated in the bottom panel of Fig. 2. Note also $\Sigma'_{c\bar{c}}(M_X + i0)$ and $\Sigma'_{c\bar{c}}(M_R - i0)$ have different signs. Since the pole now becomes quite close to the threshold, where both SRS and FRS are connected, it might have visible effects in scattering observables, though its molecular content and the square of the coupling to the $D\bar{D}^*$ scale as $\mathcal{O}(1/d^2)$. The same occurs for the $X(3872)$, which in the $d \gg d^{\mathrm{crit}}$ limit appears to be a charmonium state, mirror in the FRS of the pole found in the SRS. This behavior is in good agreement with the findings of Ref. [68] obtained using quite general arguments (see discussion after Eq. (22) of this latter reference).

The fact that in the limit $d \gg d^{\mathrm{crit}}$, both poles become dominantly charmonium can also be understood as follows. In order to keep the position of the pole corresponding to the $X(3872)$ fixed, as d increases, C_0 should also increase and take large positive values.[15] These large positive values create a strong repulsive contact force between the D and D^*

[14] Actually, the latter part of the trajectory could even be just an artifact of the model.

[15] Note that this variation of C_0 depends on the procedure used to renormalize the amplitudes. Since the position of the pole corresponding to the $X(3872)$ is fixed, from Eq. (61), one deduces that the value of $\Sigma(M_X)$ is also fixed. In the regularization scheme used in this work, G_{QM} is independent of d, and hence from Eq. (60), it is clear that, for large values of d, $C_0 \propto d^2$. Furthermore, since G_{QM} is independent of d, Eq. (69) dictates that $\Sigma'_{c\bar{c}} \propto 1/d^2$ and hence $\tilde{Z} \simeq 1$ and $\tilde{X} \simeq 0$, i.e. we have a dominantly charmonium state. An alternative scheme would be to keep C_0 fixed, but change the regularization of the loop function to keep the position of $X(3872)$ fixed. In such scheme, $G_{\mathrm{QM}} \propto \frac{1}{d^2}$, as can be seen from Eq. (60). This would be accomplished by means of an appropriate subtraction in the loop function, which would effectively account for some higher order terms in the interaction. In this scheme, $\Sigma'_{c\bar{c}} \propto d^2$, and hence $\tilde{Z} \simeq 0$ and $\tilde{X} \simeq 1$. However, one should bear in mind that the connection between the factors $\tilde{X}$ and $\tilde{Z}$ and the weights of the wave functions of the various components in the state is inspired by the findings of the work of Ref. [56,57] by Weinberg. The latter results were found within non-relativistic quantum mechanics and for weakly bound states. Undoubtedly, the connection is clearer when an UV cutoff is used to suppress the contribution of momenta much higher than the wave number associated to the bound state.

Table 2 Properties of the 2^{++} hidden charm poles as a function of d. We solve Eq. (61) with $\Lambda = 1.0$ GeV and $C_{0X}(d)$, determined from Eq. (71), can be found in Table 1. The position of the dressed $\chi_{c2}(2P)$ is fixed at $m^{\rm exp}_{\chi_{c2}} = 3927.2$ MeV in the FRS, and we also give the $X(3872)$ meson-molecular probabilities ($\tilde{X}_{X(3872)}$) for each value of d

d [fm$^{1/2}$]	$\tilde{X}_{X(3872)}$	$g^{\chi_{c2}}_{D^*\bar{D}^*}$ [GeV$^{-1/2}$]	$\tilde{X}_{\chi_{c2}}$	$\mathring{m}_{\chi_{c2}}$ [MeV]	$M_{X_2} - 2M_{D^*} - i\frac{\Gamma_{X_2}}{2}$ [MeV]	$g^{X_2}_{D^*\bar{D}^*}$ [GeV$^{-1/2}$]	$\tilde{X}_{X_2}$
0.	1	0.0	0.0	3927.2	-5.6	0.97	1.
0.05	0.98	0.27	0.01	3927.8	-4.5	0.90	0.996
0.10	0.92	0.51	0.02	3929.6	-1.8	0.67	0.991
0.15	0.84	0.69	0.04	3932.2	-0.0 at SRS	$-0.12\,i$	>1
0.20	0.75	0.82	0.05	3935.2	-6.4 at SRS	$-0.76\,i$	>1
0.22	0.71	0.86	0.06	3936.4	-21.2 at SRS	$-1.24\,i$	>1
0.25	0.66	0.90	0.06	3938.3	$-28.3 - \frac{72.9}{2}\,i$	$0.23 - 0.65\,i$	$0.47 + 0.32\,i$
0.30	0.57	0.95	0.07	3941.2	$-31.2 - \frac{162.8}{2}\,i$	$0.03 + 0.67\,i$	$0.48 - 0.04\,i$
0.35	0.49	0.96	0.07	3943.8	$-59.5 - \frac{312.6}{2}\,i$	$0.30 + 0.71\,i$	$0.52 - 0.39\,i$

mesons. This strong repulsive force, suppresses the contribution of the molecular component in the states.

Results for larger (smaller[16]) values of $\mathring{m}_{\chi_{c1}}$ are qualitatively similar, though larger (smaller) d values are needed to reach the same amount of charmonium component ($\tilde{Z}_{X(3872)} = 1 - \tilde{X}_{X(3872)}$) in the $X(3872)$.

5.1.2 *Radiative decays of the $X(3872)$ and its charmonium content*

Using vector meson dominance and assuming that the $X(3872)$ is a hadronic molecule, with the dominant component $D^0 D^{*0}$ plus a small admixture of the $\rho J/\psi$ and $\omega J/\psi$, the ratio of the $X(3872)$ branching fractions into $\psi(2S)\gamma$ and $J/\psi\gamma$ was calculated in [26] to be about 4×10^{-3}, which strongly differs from the experimental value quoted in Eq. (3). In sharp contrast, quark model calculations, assuming a $c\bar{c}\,2^3P_1$ nature for the $X(3872)$, predict a wide[17] range for this ratio, where the experimental ratio can be easily accommodated.

As mentioned in the Introduction, the study of Ref. [32] suggests that, for radiative decays of the $X(3872)$, short-range contributions are of similar importance as their long-range counter parts, and that the measured value for $R_{\psi\gamma}$ is not in conflict with a predominantly molecular nature of the $X(3872)$. Triangular $DD^{(*)}\bar{D}^{(*)}$ and $D\bar{D}^*$ loop contributions to these radiative decays were computed in [32] (Fig. 1a–e of that reference), using dimensional regularization with the $\overline{\rm MS}$ subtraction scheme at various scales $\mu = M_X/2, M_X, 2M_X$. The results of Table 2 of Ref. [32] can be summarized as follows:

$$\Gamma^{\rm loops}(X(3872) \to J/\psi\gamma) = \left(9.7 + 19.9 \log\frac{2\mu}{M_X}\right)(r_x r_g)^2\ [\text{keV}] \quad (76)$$

$$\Gamma^{\rm loops}(X(3872) \to \psi(2S)\gamma) = \left(3.8 + 1.6 \log\frac{2\mu}{M_X}\right)(r_x r'_g)^2\ [\text{keV}] \quad (77)$$

where we have adjusted the two lower values, $\mu = M_X/2$ and $\mu = M_X$, given in the table for each decay mode. The interpolating function works quite well in the case of the $\psi(2S)\gamma$ mode, while it underestimates by around 15 % the width obtained in [32] for the $J/\psi\gamma$ decay at $\mu = 2M_X$. In the above expressions, $r_x = g_{XD\bar{D}^*}/(0.97\ \text{GeV}^{-1/2})$, $r_g = g/(2\,\text{GeV}^{-3/2})$ and $r'_g = g'/(2\,\text{GeV}^{-3/2})$, with g and g', the spin-symmetric $J/\psi D^{(*)}\bar{D}^{(*)}$ and $\psi(2S)D^{(*)}\bar{D}^{(*)}$ coupling constants (see Eqs. (10)–(12) of Ref. [32]). Here we find in Tables 1 and 6, $g_{XD\bar{D}^*} = 0.90\,\text{GeV}^{-1/2}$ and $1.05\,\text{GeV}^{-1/2}$ for $\Lambda = 1$ and 0.5 GeV, respectively. Hence, the estimate taken in Ref. [32] is reasonable for the qualitative purposes of the current work. The J/ψ and $\psi(2S)$ coupling constants to the charmed mesons cannot be measured directly and are badly known. The value of $2\,\text{GeV}^{-3/2}$ for g was taken in [32] from the model estimates of Refs. [51,69]. The estimate of g' used to produce the central values of Table 2 in Ref. [32] is just an educated guess, though values of $g'/g \sim 1.67$ are justified in the analysis of Ref. [30].

The charmed meson-loop contributions to the $\Gamma(X(3872) \to \psi(nS)\gamma)$ decay show an important scale dependence, in particular in the J/ψ mode. Indeed, the ratio of the $X(3872)$ branching fractions into $\psi(2S)\gamma$ and $J/\psi\gamma$ calculated in Ref. [32] lies in the interval $(0.14\text{–}0.39)(g'/g)^2$, being the $\psi(2S)$ channel suppressed, although a lot less than claimed in Ref. [26]. (Note that values of $g'/g \sim 2$ would render the ratio to be of order one in this purely molecular picture.) This

[16] Note that Ref. [66] provides one of the smallest $\chi_{c1}(2P)$ bare masses among all recent predictions available in the literature.

[17] The results for $X(3872) \to J/\psi\gamma$ are particularly sensitive to quark model details (see for instance Table 2 of Ref. [26]).

supports the claim made in [32] that, for the radiative decays of the $X(3872)$, short-range contributions are important.

Since any physical amplitude should be independent of the scale, the dependence displayed in Eqs. (76) and (77) should be compensated by a corresponding variation in the counter-term contribution depicted in diagram 1(f) of Ref. [32]. Since the counter-terms parametrize short-range physics they may be modeled by a charm quark loop. Hence, we could estimate the size of the counter-term by employing the model presented in this work and depicted in Fig. 3.

From Eqs. (24) and (64), one trivially finds

$$\Gamma\left[X(3872)\to\psi(nS)\gamma\right] = \frac{(M_X-\mathring{m}_{\chi_{c1}})^2}{(M_X-m_{\chi_{c1}})^2+\frac{\Gamma^2_{\chi_{c1}}}{4}}\times\frac{1}{1-\Sigma'_{c\bar{c}}(M_X)} \times\frac{\delta_n^2}{3\pi}E_\gamma^3\frac{M_{\psi(nS)}}{M_X} \tag{78}$$

with $E_\gamma=(M_X^2-M^2_{\psi(nS)})/(2M_X)$. The first factor deviates from one when the width of the dressed $\chi_{c1}(2P)$ starts growing and becomes comparable with $M_X-\mathring{m}_{\chi_{c1}}$. The factor $1/(1-\Sigma'_{c\bar{c}}(M_X))$ is $\tilde{Z}_{X(3872)}=1-\tilde{X}_{X(3872)}$ (see Eq. (68)), and it can be identified with the probability to find the compact component $\chi_{c1}(2P)$ in the physical wave function of the $X(3872)$. On the other hand, the last factor is

$$\frac{\delta_n^2}{3\pi}E_\gamma^3\frac{M_{\psi(nS)}}{M_X}=\begin{cases}89\text{ keV},\ 2S\\ 60\text{ keV},\ 1S\end{cases} \tag{79}$$

using the matrix elements $\delta_{1S}=0.046\text{ GeV}^{-1}$ and $\delta_{2S}=0.38\text{ GeV}^{-1}$. We have estimated δ_{nS} from the widths given in Table III of Ref. [52] for the 2P E1 radiative transitions calculated with the non-relativistic potential model. (We have used $M_{J/\psi}=3096.92$ MeV, $M_{\psi(2S)}=3686.11$ MeV and the mass predicted in Ref. [52] for the $\chi_{c1}(2P)$ state.)

The estimate in Eq. (78) depends on the renormalization scheme and should cancel the dependence on scale of the meson-loop contributions. Here, we have computed it using an UV cutoff, $\Lambda=1$ GeV, while the meson loops were evaluated in [32] using dimension regularization with the $\overline{\text{MS}}$ subtraction scheme at $\mu=M_X/2, M_X, 2M_X$.

We pay attention to the two-meson-loop function, and compare $G_{\text{QM}}(E)/\left(4M_DM_{D^*}e^{-k^2/\Lambda^2}\right)$ (Eq. (43)), with $G^{\overline{MS}}(s,\mu)$, defined as

$$G^{\overline{MS}}(s,\mu)=i\int\frac{d^4q}{(2\pi)^4}\frac{1}{q^2-M_D^2}\frac{1}{(P-q)^2-M_{D^*}^2} =\overline{G}(s)+\frac{1}{16\pi^2}\left\{-2+\frac{1}{M_D+M_{D^*}} \times\left(M_D\log\frac{M_D^2}{\mu^2}+M_{D^*}\log\frac{M_{D^*}}{\mu^2}\right)\right\} \tag{80}$$

with P^μ the total four momentum ($P^2=s$), and the finite and scale independent function $\overline{G}(s)=G^{\overline{MS}}(s,\mu)-G^{\overline{MS}}(s=(M_D+M_{D^*})^2,\mu)$, given in Eq. (A9) of Ref. [70]. From such comparison, and looking at the FRS and in the vicinity of $s=M_X^2$, we find that scales μ of the other of M_X would correspond to UV cutoffs, Λ, much larger than 1 GeV, or equivalently $\Lambda=1$ GeV would correspond to a $\overline{MS}$ scale μ of the order of 1 GeV, significantly smaller than M_X.

We cannot increase the size of the UV cutoff within the EFT proposed in [33,34] to describe the $X(3872)$, since we will be breaking HQSS and our estimate of the counter-term will not be realistic. However, we can run down the charmed meson-loop contribution to the radiative decays calculated in [32] to scales $\mu\sim1$ GeV. In the case of the $\psi(2S)\gamma$ mode such running seems stable and leads to (Eq. (77))

$$\Gamma^{\text{loops}}(X(3872)\to\psi(2S)\gamma)\sim2.7(r_x r'_g)^2\text{ [keV] at }\mu=1\text{ GeV}, \tag{81}$$

while we will assume that the hadron loop contribution to the $X(3872)\to J/\psi\gamma$ decay is much smaller than 1 keV at scales of the order of 1 GeV, as the running in Eq. (76) seems to suggest. Thus, we consider, following the discussion in Ref. [32] (taking into account also the results of Eqs. (78) and (79)),

$$R_{\psi\gamma}(r'_g,\tilde{Z}_{X(3872)}) =\left.\frac{B_r(X\to\psi(2S)\gamma)}{B_r(X\to J/\psi\gamma)}\right|_{\text{loops + counter−term of Fig. 3}} \sim\frac{70\tilde{Z}_{X(3872)}\times f(\tilde{Z}_{X(3872)})+(1-\tilde{Z}_{X(3872)})2.7r'^2_g}{56\tilde{Z}_{X(3872)}\times f(\tilde{Z}_{X(3872)})} \tag{82}$$

where $f(\tilde{Z}_{X(3872)})$ (shown in the left panel of Fig. 4) accounts for the dressed and bare charmonium propagator ratio squared that appear in Eq. (78). The above approximation for $R_{\psi\gamma}$ only makes sense as long as $\tilde{Z}_{X(3872)}$ is larger than let us say 0.05 to justify having neglected the meson-loop contribution in the $X(3872)\to J/\psi\gamma$ mode. We have also neglected any correction due to an imprecise knowledge of the $XD\bar{D}^*$ coupling, r_x, and more importantly to possible destructive or constructive interferences between the meson-loop and the counter-term (quark-loop) contributions in the $\psi(2S)\gamma$ decay. We are aware that the latter effects might be important [30], but we cannot properly estimate them in this exploratory study, where we aim at discussing the implications of the existence of quarkonium components in the $X(3872)$ in the dynamics of the predicted $X_2(4012)$ resonance, as well as in the properties of the possible partners of these charmed resonances in the bottom sector. Note that the sign of g' is uncertain, which is also a limitation for the scheme of Ref. [30]. Moreover, we should also acknowledge that the counter-term needed in [32] might

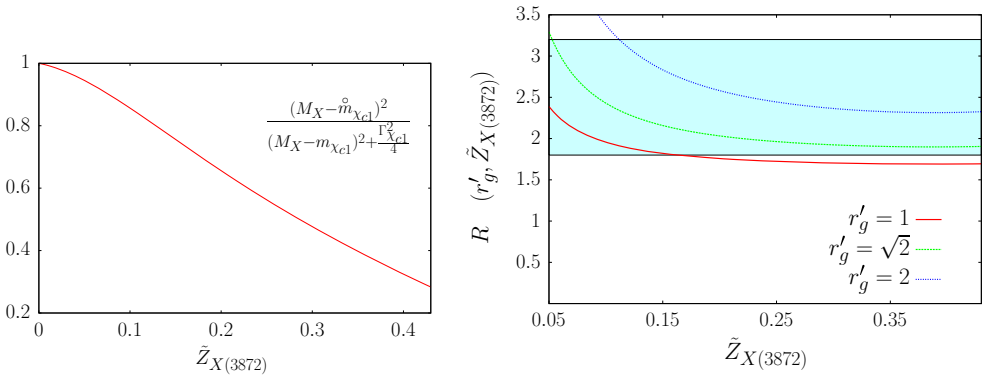

Fig. 4 Function $f(\tilde{Z}_{X(3872)})$ (*left*) entering in the definition of the ratio $R_{\psi\gamma}(r'_g, \tilde{Z}_{X(3872)})$ in Eq. (82). This latter ratio is shown in the right panel for three different values of $g' = 1, \sqrt{2}$ and 2 (units of $2\,\text{GeV}^{-3/2}$), together with the experimental band $R_{\psi\gamma} = 2.5 \pm 0.7$ from Ref. [24]. All calculations have been carried out with an UV cutoff $\Lambda = 1\,\text{GeV}$

involve contributions for other type of short-range physics, as for instance higher momentum components of the hadronic $X(3872)$ wave function. Thus, the discussion below can only be qualitative.

In the right panel of Fig. 4, the ratio $R_{\psi\gamma}(r'_g, \tilde{Z}_{X(3872)})$ is shown as a function of $Z_{X(3872)}$ for three different values of the $\psi(2S)D^{(*)}\bar{D}^{(*)}$ coupling constant, together with the experimental band given in Eq. (3) (we have added in quadratures statistical and systematic errors).

From Fig. 4, we conclude that moderate $X(3872)$ charmonium contents in the range $\tilde{Z}_{X(3872)} = 0.1 - 0.3$ lead to successful descriptions of the $R_{\psi\gamma}$ considering ratios $g'/g > 1$ in line with the expectations of Ref. [30]. Indeed, if this ratio is of the order of 2, larger $X(3872)$ charmonium contents can be easily accommodated, though in that case the experimental ratio of decay fractions of $X(3872)$ into $J/\psi\pi^+\pi^-$ and $J/\psi\pi^+\pi^-\pi^0$ final states might be difficult to be explained.

From the results in Table 1, and bearing in mind all sort of shortcomings mentioned above, we expect the mixing parameter $d(\Lambda = 1\,\text{GeV})$ to lie in the 0.1–0.25 $\text{fm}^{1/2}$ interval, which would correspond to $X(3872)$ meson-molecular probabilities in the 0.9–0.65 range.

5.1.3 Discussion

From the above considerations, the dressed charmonium state $\chi_{c1}(2P)$ should have a mass around 3910–3925 MeV, with a width in the range 5–70 MeV and a sizable molecular $(D\bar{D}^*)$ component, in the interval 6–40 %, depending on the specific value of d (see Tables 1, 6). These results are similar to those found in the quark model of Ref. [43], where charmonium and $D\bar{D}^*$ configurations are coupled using the $^3P_0$ approximation. There, the elusive $X(3872)$ meson appears as a new state with a high probability for the $D\bar{D}^*$ molecular configuration, and a sizable $c\bar{c}\,2^3P_1$ component (7–30 % depending on the strength of the used $^3P_0$ interaction). The original $\chi_{c1}(2P)$ state acquires also a sizable meson-molecular content (10–20 %), and it is identified in [43] with the $X(3940)$, whose PDG mass and width are [6] 3942 ± 9 MeV and 37^{+27}_{-17} MeV, respectively. Our predicted width for the charmonium dressed state is in good agreement with that of the $X(3940)$, though the mass is somehow low. The mass of the bare $c\bar{c}\,2^3P_1$ state used in [43] is significantly larger (3947.4 MeV) than that used here (3906 MeV), which renders the mass of the dress charmonium state in [43] naturally closer to that of the $X(3940)$ resonance. Note, however, that neither the width of the dressed $c\bar{c}\,2^3P_1$ state nor the ratio $R_{\psi\gamma}$ of $X(3872)$ radiative decays are calculated in [43]. Moreover, within the approach of the latter reference the meson loops slightly decrease the mass of the charmonium state, opposite to what we find in this work.

The phenomenological work of Ref. [30] relies in the inspired quark model findings of Ref. [10] to quantify the molecular components of the $X(3872)$, while the interplay between its charmonium and molecular components is determined from the ratio $R_{\psi\gamma}$ of radiative decays, as we have qualitatively done here. The findings of Ref. [30] favor an admixture of 5–12 % of a $\bar{c}c$ component, which can be easily accommodated within our results.

Thus, our results together with those of Refs. [30,43] do not support other interpretations of the $X(3872)$, for instance that of Ref. [71], where this resonance is described as a $c\bar{c}$ core plus higher Fock components due to the coupling to the meson–meson continuum, which is thought to be compatible with the meson $\chi_{c1}(2P)$.

5.2 Numerical results: the 2^{++} hidden charm sector

The effective interactions in the 1^{++} and 2^{++} sectors at the $X(3872)$ mass and the $D^*\bar{D}^*$ threshold are

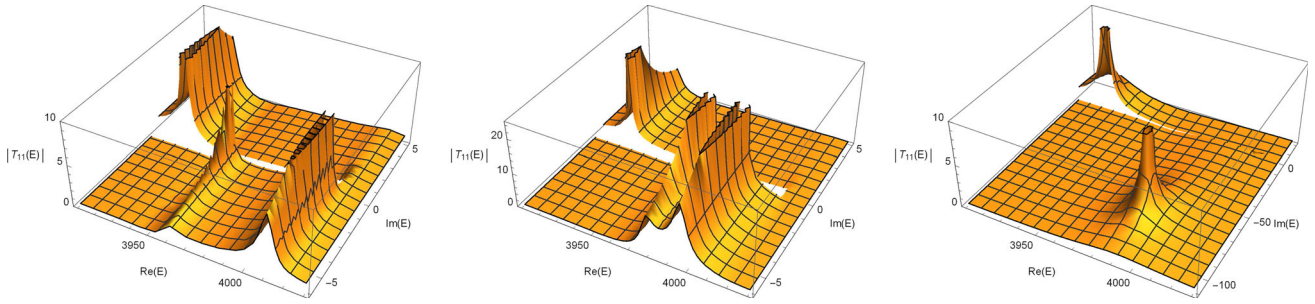

Fig. 5 Hidden charm $J^{PC} = 2^{++}$ sector. FRS ($\mathrm{Im}(E) > 0$) and SRS ($\mathrm{Im}(E) < 0$) of $|T_{11}(E)|$ [fm^2] (Eq. (59)) as a function of the complex energy E [MeV], for $d = 0.20$ (*left*), 0.22 (*middle*) and 0.25 (*right*) fm$^{1/2}$. Note that, since the T-matrix is shown for only half of the SRS (and also the FRS), the pole in the SRS conjugate to the pole shown in the figures is not visible. In the first two *plots*, there appear one pole in the FRS ($\chi_{c2}(2P)$) located at 3927.2 MeV and two more in the real axis of the SRS below threshold and disconnected from the FRS. In the *left* (*middle*) *plot*, the pole located at 4010.9 (3996.0) MeV would correspond to the $X_2(4012)$ (HQSS partner of the $X(3872)$) state, while the other one, located at 3959.5 (3978.1) MeV, arises because of the bare χ_{c2} pole included in the amplitudes. Finally in the *right plot*, there are appear the FRS $\chi_{c2}(2P)$ pole and a second one deep into the SRS complex plane. All calculations have been carried out with an UV cutoff $\Lambda = 1$ GeV. The "serrated" appearance of the poles in the first plot is due to the coarse mesh used to create the surface plot. It can be eliminated by using a finer mesh, which would require the computation of the amplitude for a larger number of complex energies

$$V_{\rm eff}^{1^{++}}(E = M_X) = C_{0X} + \frac{d^2}{M_X - \mathring{m}_{\chi_{c1}}} = \frac{1}{G_{\rm QM}(M_X)}, \quad (83)$$

$$V_{\rm eff}^{2^{++}}(E = 2M_{D^*}) = C_{0X} + \frac{d^2}{2M_{D^*} - \mathring{m}_{\chi_{c2}}}$$
$$= V_{\rm eff}^{1^{++}}(E = M_X) + d^2 \times \left(\frac{(2M_{D^*} - M_X) - (\mathring{m}_{\chi_{c2}} - \mathring{m}_{\chi_{c1}})}{(2M_{D^*} - \mathring{m}_{\chi_{c2}})(\mathring{m}_{\chi_{c1}} - M_X)} \right), \quad (84)$$

and hence $V_{\rm eff}^{2^{++}}(E) - V_{\rm eff}^{1^{++}}(E = M_X) > 0$, for E in the vicinity of the $D^*\bar{D}^*$ threshold, because we expect $(2M_{D^*} - M_X) \sim m_\pi > (\mathring{m}_{\chi_{c2}} - \mathring{m}_{\chi_{c1}})$. Indeed, for $d = d^{\rm crit}$, $C_{0X} = 0$, and thus the net interaction in the 2^{++} sector will be repulsive since $2M_{D^*} > \mathring{m}_{\chi_{c2}}$.

In the following, we will fix $\mathring{m}_{\chi_{c2}}$ such that the dressed $2P$ quarkonium mass ($m_{\chi_{c2}}$) will be equal to $m_{\chi_{c2}}^{\rm exp}$. In Table 2, we show the properties of the poles found in the 2^{++} hidden charm sector as a function of the mixing LEC d. We solve Eq. (61) with an UV cutoff of 1 GeV as in the case of Table 1. First, we see that $\mathring{m}_{\chi_{c2}}$ and $m_{\chi_{c2}}^{\rm exp}$ differ just by a few MeVs, and hence we check that the $D^*\bar{D}^*$ loops have little influence on the charmonium level, though it develops a sizable coupling to the meson pair. Moreover, $\mathring{m}_{\chi_{c2}} > m_{\chi_{c2}}^{\rm exp}$, since $\Sigma_{c\bar{c}}(m_{\chi_{c2}}^{\rm exp}) < 0$ in the FRS and for this regime of C_{0X} values and energies. As d increases, the molecular $X_2(4012)$ (HQSS partner of the $X(3872)$) state approaches to $2M_{D^*}$, and for $d > 0.15$ fm$^{1/2}$ it crosses to the SRS, moving quickly away from threshold along the real axis.[18] Actually, what happens is that the $X_2(4012)$ pole at the SRS merges with a replica of the bare $\chi_{c2}(2P)$ pole, as illustrated in Fig. 5, and the new pole gets deep into the complex plane when d increases above 0.22 fm$^{1/2}$.

From the above discussion of the $X(3872)$ radiative decays, we expect the mixing LEC d to take values in the range 0.1–0.25 fm$^{1/2}$ for $\Lambda = 1$ GeV, which in turn would imply that the $X_2(4012)$ would likely lie in the SRS, below threshold disconnected from the FRS, either in the real axis or deep into the complex plane. Note that, for values of d close to $d \simeq 0.15$ fm$^{1/2}$, even in cases where the pole is in the SRS below threshold, it could, however, have sizable effects on the observables, since it would be close to the $D^*\bar{D}^*$ threshold, where SRS and FRS are connected. Considering equivalent molecular components of the $X(3872)$, the conclusions obtained with $\Lambda = 0.5$ GeV are qualitatively similar, as can be seen in Table 6.[19]

Thus, the different interplay of the charmonium components in the $X(3872)$ and in its hypothetical 2^{++} HQSS partner makes plausible that the latter state is not accessible to the direct observation, or, in other words, that it does not

[18] Note that $\Sigma_{c\bar{c}}(E) > 0$ in the SRS, for real energies below $2M_{D^*}$ and d around 0.15 fm$^{1/2}$ because the loop factor $(1 - C_{0X} G_{\rm QM}^{II})$ takes negative values.

[19] The $\Lambda = 0.5$ and $\Lambda = 1$ GeV X_2 predicted masses, calculated neglecting the quarkonium mixing ($d = 0$), are similar (they differ by less than 1 MeV) and for $d = 0$ the X_2 state would be located around 5 MeV below the $D^*\bar{D}^*$ threshold. The $\chi_{c2}(2P)$ is much lighter, around 85–90 MeV, and in this case the form factor f_Λ that appears in Eq. (63) is around twice larger for $\Lambda = 0.5$ GeV than for $\Lambda = 1$ GeV. We see this dependence on the UV cutoff in $g_{D^*\bar{D}^*}^{\chi_{c2}}$, coupling of the $\chi_{c2}(2P)$ state to the $D^*\bar{D}^*$ meson pair, which for similar molecular components of the $X(3872)$ is around 2–3 times larger for $\Lambda = 0.5$ GeV than when it is calculated using $\Lambda = 1$ GeV, reflecting a large off-shell ambiguity for this coupling. This cutoff dependence cancels out for instance in the completeness relation of Eq. (66) or in the relation among quarkonium and meson–molecular couplings of Eq. (70).

Table 3 Masses of several hidden bottom states and thresholds in MeV. We use the isospin averaged B-meson mass, $M_B = 5279.40$ MeV, and for the vector meson we take $M_{B^*} = 5324.83$ MeV [6]. The X_b and X_{b2} are heavy-quark spin–flavor partners of the $X(3872)$ predicted in [36]. We quote here the masses found in this reference for Λ =1 and 0.5 GeV, and the errors account for heavy-quark symmetry breaking corrections. The masses of the $\chi_{bJ}(nP)$ are taken from the PDG [6], with errors added in quadratures, except for that of the 2^{++} 3P state. † : Theory predictions for the $\chi_{b2}(3P) - \chi_{b1}(3P)$ mass splitting vary from 8 to 12 MeV [72–74]. We set here this splitting to 10 MeV

1^{++}			2^{++}		
State	Mass	$B\bar{B}^*$ threshold	State	Mass	$B^*\bar{B}^*$ threshold
X_b ($\Lambda = 1$ GeV) [36]	10539^{+25}_{-27}	10604.2	$X_{b2}(\Lambda = 1\,\text{GeV})$ [36]	10584^{+25}_{-27}	10649.7
X_b ($\Lambda = 0.5$ GeV) [36]	10580^{+9}_{-8}		$X_{b2}(\Lambda = 0.5\,\text{GeV})$ [36]	10626^{+8}_{-9}	
$\chi_{b1}(1P)$	9892.78 ± 0.40		$\chi_{b2}(1P)$	9912.21 ± 0.40	
$\chi_{b1}(2P)$	10255.46 ± 0.55		$\chi_{b2}(2P)$	10268.65 ± 0.55	
$\chi_{b1}(3P)$	10512.1 ± 2.3		$\chi_{b2}(3P)$	$10522.1^{\dagger}$	

exist as an actual QCD state.[20] Within the model developed in Ref. [43], it is also found insufficient attraction in the 2^{++} sector to create an additional, mostly $D^*\bar{D}^*$ molecular, state [44]. Moreover, we should remind the reader here that in the scheme of Ref. [45], mass and width of this state were strongly affected by the one-pion exchange interaction in coupled channels.

This state in the 2^{++} sector was predicted in [33,34,36], where it was also shown that even considering 15–20 % HQSS violations its existence seemed to be granted. However, the $X_2(4012)$ has not been observed yet, and hence the study carried out here might shed light on this issue. This also shows that corrections stemming from charmonium admixture in the molecular $X(3872)$, enhanced/distorted by threshold effects, need to be explicitly considered exhibiting their energy dependence, and they cannot be just accounted for in the short-distance meson–meson LECs.

5.3 Numerical results: the hidden bottom 1^{++} and 2^{++} sectors

In Table 3, we compile the masses of the bottomonium states quoted in the PDG in the 1^{++} and 2^{++} sectors, together with those of the hidden bottom partners of the $X(3872)$ and the $X_2(4012)$ predicted in [36]. As we warned the reader in the introduction, the bottom and charm sectors were connected in [36] by assuming the bare couplings in the $4H$ interaction Lagrangian of Eq. (16) to be independent of the heavy-quark mass. Neither the X_b, nor the X_{b2} have been observed yet, as it happens for the $X_2(4012)$. Moreover, their predicted masses show an important UV-cutoff dependence. We first focus on the $\Lambda = 1$ GeV case because for this value of the UV cutoff, the predicted binding energies of both X_b and X_{b2} are much larger than those obtained in the $\Lambda = 0.5$ GeV case ($\simeq 65$ MeV versus $\simeq 25$ MeV). Nevertheless results for the latter UV cutoff can be found in the appendix, and it will be considered for the general discussion.

We fix $\overset{\circ}{m}_{\chi_{b1}}$ and $\overset{\circ}{m}_{\chi_{b2}}$ by requiring that the dressed quarkonium masses $m_{\chi_{bJ}}$ will match those of the $3P$ states quoted in Table 3. The bare states lie below the X_b and X_{b2} states, which produces some repulsion, as in the case of the hidden charm X_2 state. Constituent quark models predict additional bottomonium states. Here, we pay attention to the spectrum obtained in the recent work of Ref. [74], where the nonrelativistic $Q\bar{Q}$ interaction used in Ref. [43] is employed and a global agreement with the experimental pattern is found. Among the higher levels reported in [74], the $4\,^3P_1(10737)$, $2\,^3F_2(10569)$, $4\,^3P_2(10744)$ and $3\,^3F_2(10782)$ might have some relevance for the present discussion [44]. The $4P$ states are heavier than the X_b and X_{b2}, and they are located around 130 and 95 MeV above the $B\bar{B}^*$ and $B^*\bar{B}^*$ thresholds, respectively. These levels would produce extra attractions. On the other hand and because of the large orbital angular momentum, the F-states in the 2^{++} sector seem to play a really sub-dominant role [44] in the dynamics of the X_{b2}. We will examine here the worst of the scenario for the existence of the X_b and X_{b2} states, and we will consider only the $3P$ states, neglecting any attraction from the $4P$ bottomonia.

The contact interaction term C_{0X} is fixed from the $X(3872)$ mass, and thus its magnitude depends on the LEC d that mixes the molecular $D\bar{D}^*$ and $\chi_{c1}(2P)$ components. The presence of the charmonium state provides an effective attraction that contributes to binding the $X(3872)$, which translates in a smaller $|C_{0X}|$, as seen in Tables 1 and 6 for $\Lambda = 1$ and 0.5 GeV, respectively. Assuming the same value for C_{0X} in the bottom sector, we still need to determine the mixing parameter in the bottom sector (d^{bottom}), which as discussed in Sect. 5.3 depends in principle on the heavy-quark flavor. Through this LEC, the $3P$ bottomonium states will produce some repulsion in the effective $B^{(*)}\bar{B}^{(*)}$ interaction.

[20] This is somewhat an abuse of language. We call "actual QCD states" states that produce observable effects. If a SRS pole is located below threshold but deep in the complex plane, or it is close to the real axis, but much below the threshold, it will not produce any observable effects, and hence it will be impossible to detect.

Table 4 Properties of the 1^{++} hidden bottom poles as a function of d. We solve Eq. (61) with $\Lambda = 1.0\,\text{GeV}$ and $C_{0X}(d)$, determined from Eq. (71), can be found in Table 1. The position of the dressed $\chi_{b1}(3P)$ is fixed at $m^{\text{exp}}_{\chi_{b1}} = 10512.1\,\text{MeV}$ in the FRS, and we also give the $X(3872)$ meson-molecular probabilities ($\tilde{X}_{X(3872)}$) for each value of d

d [fm$^{1/2}$]	$\tilde{X}_{X(3872)}$	$g^{\chi_{b1}}_{B\bar{B}^*}$ [GeV$^{-1/2}$]	$\tilde{X}_{\chi_{b1}}$	$\mathring{m}_{\chi_{b1}}$ [MeV]	$E_{X_b} - M_B - M_{B^*}$ [MeV]	$g^{X_b}_{B\bar{B}^*}$ [GeV$^{-1/2}$]	$\tilde{X}_{X_b}$
0.	1	0.0	0.0	10512.1	−65.9	2.30	1.
0.05	0.98	0.98	0.09	10515.0	−60.7	2.04	0.91
0.10	0.92	1.46	0.20	10521.4	−47.6	1.55	0.80
0.15	0.84	1.59	0.24	10527.8	−30.8	1.11	0.77
0.20	0.75	1.57	0.23	10532.6	−13.1	0.69	0.80
0.25	0.66	1.49	0.21	10536.1	−0.1	0.16	0.96
0.30	0.57	1.40	0.18	10538.5	$4.9 - \frac{68.2}{2}\,i$	$0.05 - 0.26\,i$	$0.43 + 0.16\,i$
0.35	0.49	1.29	0.16	10540.2	$44.8 - \frac{181.4}{2}\,i$	$0.12 + 0.28\,i$	$0.55 - 0.21\,i$

For practical purposes, we will assume the mixing of molecular and quarkonium components independent of both flavor and the $Q\bar{Q}$ radial[21] quantum number in the heavy-quark limit. Even if inexact, these assumptions will allow us, at least qualitatively, to obtain an idea of the effects of quarkonium-molecular configurations admixtures on the X_b and X_{b2} states. Thus and from the discussion in Sect. 5.1.2, we consider the C_{0X} values fixed from the $X(3872)$, and associated to $d(\Lambda = 1\,\text{GeV})$ in the range 0.1–0.25 fm$^{1/2}$, and we use the same values for $d^{\text{bottom}}(\Lambda = 1\,\text{GeV})$ to take into account the repulsion induced by the $\chi_{b1}(3P)$ and $\chi_{b2}(3P)$ states. Pole positions calculated using $\Lambda = 1$ GeV and different values of the mixing parameter d are presented in Tables 4 and 5 for the 1^{++} and 2^{++} sectors, respectively. The d-dependence is quite similar in the two sectors and it is mostly dictated by the proximity of the resonances to the bottomonium levels. We find moderate bare–dressed quarkonium mass differences of the order 5–25 [5–20] MeV, and molecular meson contents in the dressed state ranging in the interval 10–20 % [5–10 %] for the $\chi_{b1}(3P)$ [$\chi_{b2}(3P)$] state. On the other hand, we see that as long the $X(3872)$ meson-molecular component is larger than 65 % ($\tilde{Z}_{X(3872)} < 35$ %), both the X_b and the X_{b2} states should exist and should be observed in future experiments. However, the different interplay of the quarkonium components in the $X(3872)$ and in its hypothetical 1^{++} and 2^{++} hidden bottom partners produces significant changes in the masses of the latter states. Thus, instead of bindings of the order of 65 MeV, we would expect the molecular bottom states to lie still below, but much closer to their respective two-meson thresholds, about 45–50 MeV at most.[22] Indeed, for the largest considered admixtures, $d(\Lambda = 1\,\text{GeV}) = 0.2$–$0.25\,\text{fm}^{1/2}$, the X_b and X_{b2} could have binding energies of only few MeV or less.

Results obtained using $\Lambda = 0.5\,\text{GeV}$ are presented in the Table 7 of the appendix. Besides the trivial dependence of the mixing parameter d, and of $g^{\chi_{b1}}_{B\bar{B}^*}$ and $g^{\chi_{b2}}_{B\bar{B}^*}$ on the UV cutoff,[23] the conclusions are qualitatively similar to those discussed above in the $\Lambda = 1\,\text{GeV}$ case. Thus, we find also now moderate bare–dressed quarkonium mass differences, though smaller than for $\Lambda = 1\,\text{GeV}$, as it also occurs for the molecular meson contents of the $\chi_{bJ}(3P)$ dressed states. For $X(3872)$ meson–molecular components larger than 65 % ($\tilde{Z}_{X(3872)} < 35\%$), both the X_b and the X_{b2} should also exist when $\Lambda = 0.5\,\text{GeV}$ is used, though they would be less bound than in the $\Lambda = 1\,\text{GeV}$ case, and for the smallest $X(3872)$ molecular component scenarios, these states would appear now as poles in the SRS, located relatively close to their respective thresholds. Moreover, as long as the X_b and X_{b2} would remain bound, they would present mostly a molecular nature, with quarkonium $b\bar{b}\,3^3P_{1,2}$ components quite small ($\leq 5\,\%$) and less important than in the $\Lambda = 1$ GeV case, where the quarkonium probabilities could be larger, even of the order of 10 or 20 %. If the poles show up in the SRS, their molecular contents turn out to be greatly reduced.

The 1^{++} and 2^{++} hidden bottom sectors were analyzed in Ref. [44] within the quark model of Ref. [43]. As mentioned earlier, the $^3P_0$ phenomenological approximation is

[21] Note that in charmonium, we considered the $c\bar{c}$ pair in the $2P$ wave, while in bottomonium, the $3P$-states would be the closest ones to the X_b and X_{b2} resonances.

[22] The heavy-quark symmetry breaking uncertainties quoted in Table 3 for these states would account to a great extent for the changes induced by charmonium contents of the $X(3872)$ smaller than 10–15 %.

[23] In the case of the couplings, it is mostly due to the factor f_Λ that appears in their definition in Eq. (63), as we already discussed for the case of the $\chi_{c2}(2P)$. Indeed in the hidden bottom sector, the quarkonium $b\bar{b}\,3^3P_{1,2}$ states are located well below ($\simeq$ 90 and 130 MeV, respectively) their respective two-meson thresholds, and f_Λ induces a large dependence of the couplings on Λ, around a factor of 4 in the 1^{++} sector and of 8 in the 2^{++} one.

Table 5 Properties of the 2^{++} hidden bottom poles as a function of d. We solve Eq. (61) with $\Lambda = 1.0\,\text{GeV}$ and $C_{0X}(d)$, determined from Eq. (71), can be found in Table 1. The position of the dressed $\chi_{b2}(3P)$ is fixed at $m^{\text{exp}}_{\chi_{b2}} = 10522.1\,\text{MeV}$ in the FRS, and we also give the $X(3872)$ meson-molecular probabilities ($\tilde{X}_{X(3872)}$) for each value of d

d [fm$^{1/2}$]	$\tilde{X}_{X(3872)}$	$g^{\chi_{b2}}_{B^*\bar{B}^*}$ [GeV$^{-1/2}$]	$\tilde{X}_{\chi_{b2}}$	$\mathring{m}_{\chi_{b2}}$ [MeV]	$E_{X_{b2}} - 2M_{B^*}$ [MeV]	$g^{X_{b2}}_{B^*\bar{B}^*}$ [GeV$^{-1/2}$]	$\tilde{X}_{X_{b2}}$
0.	1	0.0	0.0	10522.1	-66.2	2.31	1.
0.05	0.98	0.69	0.02	10523.4	-62.5	2.17	0.98
0.10	0.92	1.20	0.06	10526.9	-52.3	1.82	0.94
0.15	0.84	1.50	0.10	10531.3	-37.2	1.37	0.91
0.20	0.75	1.64	0.11	10535.7	-19.4	0.90	0.90
0.25	0.66	1.67	0.12	10539.5	-3.1	0.41	0.93
0.30	0.57	1.64	0.11	10542.5	$-18.0 - \frac{37.4}{2}\,i$	$0.16 - 0.28\,i$	$0.46 + 0.75\,i$
0.35	0.49	1.59	0.11	10545.0	$27.1 - \frac{195.1}{2}\,i$	$0.09 + 0.28\,i$	$0.57 - 0.15\,i$

employed in [44] to couple quarkonium and two-meson degrees of freedom. As argued here, for $J^{PC} = 1^{++}$ some repulsion from the bottomonium state below the $B\bar{B}^*$ threshold is found in [44], but, however, there, it is not given a definitive answer to the existence or not existence of the X_b state, since the results of that work depends critically of the strength parameter of the $^3P_0$ model within its uncertainties. In any case, its existence is not discarded. In the 2^{++} sector, an additional state, with a mass of 10648 MeV is found in [44], and it is pointed out that there is a similar repulsion and attraction from the states below $(3P)$ and above $(4P)$ threshold. This state would be just 1 or 2 MeV below the $B^*\bar{B}^*$ threshold, and it could be easily accommodated within our expectations.

6 Conclusions

In this work, we have set up a scheme based on HQSS to study quarkonium admixtures in molecular states like the $X(3872)$ or its heavy-quark spin–flavor partners, X_2, X_b and X_{b2}, not discovered yet. We have discussed how the interplay of the charmonium components in the $X(3872)$ produces an extra attraction, and thus we have argued that one would need less attractive meson–meson interactions to bind the state. Such an attraction does not appear in the 2^{++} sector, where one should expect instead some repulsion from the charmonium degrees of freedom. The 1^{++} bare charmonium pole would be modified due to the $D\bar{D}^{(*)}$ loop effects, and it would be moved to the complex plane acquiring also a finite width. Despite having neglected isospin breaking terms and working at LO in the heavy-quark expansion, these effects still depend on two unknowns LEC's. The mass of the $X(3872)$ imposes a relation among them, and we have considered the ratio $R_{\psi\gamma}$ of the $X(3872)$ branching fractions into $J/\psi\gamma$ or $\psi(2S)\gamma$ to further constrain the range of variation of these two LEC's. To that end, we have used the EFT prediction for $R_{\psi\gamma}$ obtained in Ref. [32], where meson–loop contributions were calculated, and complemented it with the quark–loop contribution driven by the $X(3872) \to \chi_{c1}(2P)$ transition derived here. We have found that around a 10–30 % charmonium probability (estimated by means of the compositeness sum rule of Eq. (53)) in the $X(3872)$ might explain the experimental value of the ratio $R_{\psi\gamma}$, confirming that this ratio is not in conflict with a predominantly molecular nature of the $X(3872)$. In turn, the dressed $\chi_{c1}(2P)$ would have a mass and a width, which would make plausible its identification with the $X(3940)$ resonance.

For 10–30 % $c\bar{c}\,2\,^3P_1$ content in the $X(3872)$, the X_2 resonance destabilizes and disappears from the spectrum, becoming either a virtual state or being located deep into the complex plane, with decreasingly influence in the $D^*\bar{D}^*$ scattering line. The crucial point here is that the $\chi_{c2}(2P)$ state is located well below the expected mass of the X_2 in the vicinity of the $D^*\bar{D}^*$ threshold. In sharp contrast to what happens in the $X(3872)$ sector, where the $\chi_{c1}(2P)$ is close (but above) to the two-meson threshold, the $\chi_{c2}(2P)$ produces a meson–meson repulsive interaction. The $X_2(4012)$ has not been observed yet, contrary to the HQSS expectations [36], and thus the study carried out here might help to understand this fact, because we have shown that this resonance might not be accessible to the direct observation.

In the hidden bottom sectors and despite the changes induced by the quarkonium admixtures, it is reasonable to expect that both X_b and X_{b2} resonances might be observed in the short future. Nevertheless, we should remind the reader here once more that our conclusions in the bottom sector rely on the assumption that the contact term in the $4H$ Lagrangian and the LEC d, which controls the admixtures of quarkonium and two-meson configurations, are independent of the heavy flavor. Moreover, we have also assumed that the latter parameter does not depend on the $Q\bar{Q}$ radial configuration.

Hence, it is difficult to estimate the systematic uncertainties that affect our analysis of the X_b and X_{b2} resonances. However one should bear in mind, in sharp contrast with the $\chi_{c1}(2P) - X(3872)$ case, the bottomonium states are far ($\simeq 100\,\text{MeV}$) from the $B^{(*)}\bar{B}^{(*)}$ thresholds. Thus, it seems reasonable that effects due to the extra repulsion induced by the $3P$ bottomonia in the X_b and X_{b2} molecular states, when they are placed close to their respective two-meson thresholds, should not play a role as important as in the $X(3872)$.

The picture that comes out from our study turns out to be in a remarkable agreement, at least qualitatively, with the findings of the quark model of Refs. [43,44]. In this work, the $^3P_0$ phenomenological approximation is employed to couple quarkonium and two-meson degrees of freedom. Thus, the X_2 state is not found in [43], while the $X(3872)$ emerges with a charmonium content similar to that favored by our study of its radiative decays. In the 2^{++} hidden bottom sector, an additional state with a mass of 10648 MeV is reported in [44]. Such state would correspond to the X_{b2}, and this mass could be accommodated within our predictions. In the 1^{++} sector, the quark model does not provide a definite answer about the the existence of the X_b, since the results of Ref. [44] depends critically of the strength parameter of the $^3P_0$ model within its uncertainties.

Acknowledgments We would like to thank M. Albaladejo, D.R. Entem, P. Fernández-Soler, F.-K. Guo and J.A. Oller for enlightening comments. This research has been supported by the Spanish Ministerio de Economía y Competitividad and European FEDER funds under the Contracts FIS2014-51948-C2-1-P, FIS2014-57026-REDT and SEV-2014-0398, by Generalitat Valenciana under Contract PROMETEOII/2014/0068 and by TUBITAK under Contract 114F234.

Funded by SCOAP[3].

Appendix A: UV $\Lambda = 500$ MeV results

In this appendix, we compile the properties of the 1^{++} and 2^{++} hidden charm (Table 6) and hidden bottom (Table 7) poles as a function of the mixing LEC d, when an UV cutoff $\Lambda = 0.5\,\text{GeV}$ is used to regularized the $4H$-interactions. These results complement to those collected in Tables 1, 2, 4 and 5, which were obtained with $\Lambda = 1\,\text{GeV}$.

Table 6 Properties of the 1^{++} and 2^{++} hidden charm poles as a function of d. We solve Eq. (61) with $\Lambda = 0.5\,\text{GeV}$ and for each value of d, C_{0X} is determined from Eq. (71). The position of the $X(3872)$ is fixed at $M_X = 3871.69\,\text{MeV}$ in the FRS. The $\chi_{c1}(2P)$ pole is located in the SRS, while the position of the dressed $\chi_{c2}(2P)$ is fixed at $m_{\chi_{c2}}^{\text{exp}} = 3927.2\,\text{MeV}$ in the FRS. Finally, $B_{X_2} = M_{X_2} - 2M_{D^*} - i\frac{\Gamma_{X_2}}{2}$ and $d^{\text{crit}}(\Lambda = 0.5\,\text{GeV}) = \sqrt{\frac{M_X - \mathring{m}_{\chi_{c1}}}{G_{\text{QM}}^I(M_X)}} = 0.580\,\text{fm}^{1/2}$

d	C_{0X}	$X(3872)$		$\chi_{c1}(2P)$			$\chi_{c2}(2P)$			X_2		
		$g_{D\bar{D}^*}^{X(3872)}$	$\tilde{X}$	$(m_{\chi_{c1}}, \Gamma_{\chi_{c1}})$	$g_{D\bar{D}^*}^{\chi_{c1}}$	$\tilde{Z}$	$g_{D^*\bar{D}^*}^{\chi_{c2}}$	$\tilde{X}$	$\mathring{m}_{\chi_{c2}}$	B_{X_2}	$g_{D^*\bar{D}^*}^{X_2}$	$\tilde{X}$
$[\text{fm}^{1/2}]$	$[\text{fm}^2]$	$[\text{GeV}^{-1/2}]$		[MeV]	$[\text{GeV}^{-1/2}]$		$[\text{GeV}^{-1/2}]$		[MeV]	[MeV]	$[\text{GeV}^{-1/2}]$	
0	−1.94	1.05	1	(3906, 0)	0	1	0	0	3927.2	−4.8	1.10	1
0.1	−1.88	1.04	0.98	(3906.7, 1.5)	$0.06 + 0.13\,i$	$0.99 + 0.01\,i$	0.66	0.0	3927.7	−3.9	1.00	1.00
0.2	−1.71	1.02	0.93	(3908.8, 6.3)	$0.13 + 0.24\,i$	$0.96 + 0.05\,i$	1.26	0.02	3928.9	−1.7	0.73	0.99
0.3	−1.42	0.98	0.86	(3912.3, 15.6)	$0.21 + 0.33\,i$	$0.92 + 0.11\,i$	1.77	0.03	3930.9	−0.0 at SRS	$-0.08\,i$	>1
0.4	−1.02	0.93	0.78	(3917.5, 31.9)	$0.30 + 0.40\,i$	$0.87 + 0.21\,i$	2.16	0.05	3933.2	−8.3 at SRS	$-0.69\,i$	>1
0.5	−0.50	0.87	0.69	(3925.4, 61.2)	$0.41 + 0.45\,i$	$0.77 + 0.37\,i$	2.44	0.06	3935.7	$-10.6 - \frac{102.6\,i}{2}$	$0.05 + 0.49\,i$	$0.53 + 0.01\,i$
d^{crit}	0.0	0.83	0.62	(3938.6, 102.6)	$0.51 + 0.51\,i$	$0.57 + 0.56\,i$	2.60	0.07	3937.8	$27.7 - \frac{181.9\,i}{2}$	$0.26 + 0.55\,i$	$0.77 - 0.25\,i$
0.7	0.88	0.77	0.53	(3809.7,0) at SRS	0.38	1.36	2.74	0.08	3940.7	$107.9 - \frac{187.8\,i}{2}$	$0.37 + 0.57\,i$	$0.94 - 0.12\,i$

Table 7 Properties of the 1^{++} and 2^{++} hidden bottom poles as a function of d. We solve Eq. (61) with $\Lambda = 0.5\,\text{GeV}$ and $C_{0X}(d)$, determined from Eq. (71), can be found in Table 6. The position of the dressed $\chi_{b1}(3P)$ and $\chi_{b2}(3P)$ are fixed at 10512.1 and 10522.1 MeV in the FRS. The positions of the X_b and X_{b2} poles are determined by $B_{X_b} = M_{X_b} - M_B - M_{B^*} - i\frac{\Gamma_{X_b}}{2}$ and $B_{X_{b2}} = M_{X_{b2}} - 2M_{B^*} - i\frac{\Gamma_{X_{b2}}}{2}$, respectively. The LEC $d^{\text{crit}}(\Lambda = 0.5\,\text{GeV}) = 0.580\,\text{fm}^{1/2}$ reproduces the mass of the $X(3872)$ with $C_{0X} = 0$ and $\Lambda = 0.5\,\text{GeV}$. Note that we also give the $X(3872)$ meson-molecular probabilities ($\tilde{X}_{X(3872)}$) for each value of d

d [fm$^{1/2}$]	$\tilde{X}_{X(3872)}$	$\chi_{b1}(3P)$			X_b			$\chi_{b2}(3P)$			X_{b2}		
		$g^{\chi_{b1}}_{B\bar{B}^*}$ [GeV$^{-1/2}$]	$\tilde{X}$	$\mathring{m}_{\chi_{b1}}$ [MeV]	B_{X_b} [MeV]	$g^{X_b}_{B\bar{B}^*}$ [GeV$^{-1/2}$]	$\tilde{X}$	$g^{\chi_{b2}}_{B^*\bar{B}^*}$ [GeV$^{-1/2}$]	$\tilde{X}$	$\mathring{m}_{\chi_{b2}}$ [MeV]	$B_{X_{b2}}$ [MeV]	$g^{X_{b2}}_{B^*\bar{B}^*}$ [GeV$^{-1/2}$]	$\tilde{X}$
0	1	0	0	10512.1	−24.2	2.43	1	0	0	10522.1	−24.2	2.44	1
0.1	0.98	2.60	0.01	10512.8	−22.3	2.21	0.99	4.91	0.0	10522.6	−22.6	2.24	1.0
0.2	0.93	4.85	0.03	10514.7	−16.9	1.65	0.97	9.32	0.02	10523.8	−17.7	1.74	0.99
0.3	0.86	6.56	0.06	10517.4	−8.9	0.96	0.95	13.04	0.03	10525.8	−10.3	1.08	0.97
0.4	0.78	7.72	0.08	10520.4	−0.8	0.30	0.96	15.92	0.04	10528.2	−2.1	0.43	0.97
0.5	0.69	8.42	0.10	10523.6	$3.2 - \frac{48.2\,i}{2}$	$0.02 + 0.20\,i$	$0.57 + 0.07\,i$	17.99	0.06	10530.7	$-13.7 - \frac{30.3\,i}{2}$	$-0.06 + 0.20\,i$	$0.55 + 0.52\,i$
d^{crit}	0.62	8.72	0.10	10526.0	$41.6 - \frac{63.6\,i}{2}$	$0.14 + 0.21\,i$	$0.82 - 0.12\,i$	19.13	0.06	10532.8	$35.6 - \frac{71.2\,i}{2}$	$0.12 + 0.21\,i$	$0.86 - 0.09\,i$
0.7	0.53	8.87	0.11	10529.1	$81.5 - \frac{43.3\,i}{2}$	$0.19 + 0.14\,i$	$0.90 - 0.06\,i$	20.13	0.07	10535.7	$78.1 - \frac{46.9\,i}{2}$	$0.18 + 0.15\,i$	$0.93 - 0.04\,i$

References

1. S.K. Choi et al. (Belle), Phys. Rev. Lett. **91**, 262001 (2003). doi:10.1103/PhysRevLett.91.262001. arXiv:hep-ex/0309032 [hep-ex]
2. D. Acosta et al. (CDF), Phys. Rev. Lett. **93**, 072001 (2004). doi:10.1103/PhysRevLett.93.072001. arXiv:hep-ex/0312021 [hep-ex]
3. V.M. Abazov et al. (D0), Phys. Rev. Lett. **93**, 162002 (2004). doi:10.1103/PhysRevLett.93.162002. arXiv:hep-ex/0405004 [hep-ex]
4. B. Aubert et al. (BaBar), Phys. Rev. **D71**, 071103 (2005). doi:10.1103/PhysRevD.71.071103. arXiv:hep-ex/0406022 [hep-ex]
5. R. Aaij et al. (LHCb), Eur. Phys. J. **C72**, 1972 (2012). doi:10.1140/epjc/s10052-012-1972-7. arXiv:1112.5310 [hep-ex]
6. K.A. Olive et al., Particle Data Group. Chin. Phys. C **38**, 090001 (2014). doi:10.1088/1674-1137/38/9/090001
7. R. Aaij et al. (LHCb). Phys. Rev. Lett. **110**, 222001 (2013). doi:10.1103/PhysRevLett.110.222001. arXiv:1302.6269 [hep-ex]
8. T. Barnes, S. Godfrey, Phys. Rev. D **69**, 054008 (2004). doi:10.1103/PhysRevD.69.054008. arXiv:hep-ph/0311162 [hep-ph]
9. M. Suzuki, Phys. Rev. D **72**, 114013 (2005). doi:10.1103/PhysRevD.72.114013. arXiv:hep-ph/0508258 [hep-ph]
10. E.S. Swanson, Phys. Lett. B **588**, 189 (2004). doi:10.1016/j.physletb.2004.03.033. arXiv:hep-ph/0311229 [hep-ph]
11. M.B. Voloshin, Phys. Lett. B **604**, 69 (2004). doi:10.1016/j.physletb.2004.11.003. arXiv:hep-ph/0408321 [hep-ph]
12. E. Braaten, M. Kusunoki, Phys. Rev. D **72**, 054022 (2005). doi:10.1103/PhysRevD.72.054022. arXiv:hep-ph/0507163 [hep-ph]
13. D. Gamermann, E. Oset, Eur. Phys. J. A **33**, 119 (2007). doi:10.1140/epja/i2007-10435-1. arXiv:0704.2314 [hep-ph]
14. X. Liu, Y.-R. Liu, W.-Z. Deng, S.-L. Zhu, Phys. Rev. D **77**, 034003 (2008). doi:10.1103/PhysRevD.77.034003. arXiv:0711.0494 [hep-ph]
15. Y.-R. Liu, X. Liu, W.-Z. Deng, S.-L. Zhu, Eur. Phys. J. C **56**, 63 (2008). doi:10.1140/epjc/s10052-008-0640-4. arXiv:0801.3540 [hep-ph]
16. Y.-B. Dong, A. Faessler, T. Gutsche, V.E. Lyubovitskij, Phys. Rev. D **77**, 094013 (2008). doi:10.1103/PhysRevD.77.094013. arXiv:0802.3610 [hep-ph]
17. D. Gamermann, J. Nieves, E. Oset, E. Ruiz Arriola, Phys. Rev. D **81**, 014029 (2010). doi:10.1103/PhysRevD.81.014029. arXiv:0911.4407 [hep-ph]
18. K. Abe et al. (Belle), in *Lepton and photon interactions at high energies. Proceedings, 22nd International Symposium, LP 2005, Uppsala, Sweden, June 30–July 5, 2005* (2005). arXiv:hep-ex/0505037 [hep-ex]
19. P. del Amo Sanchez et al. (BaBar), Phys. Rev. **D82**, 011101 (2010). doi:10.1103/PhysRevD.82.011101. arXiv:1005.5190 [hep-ex]
20. S.K. Choi et al., Phys. Rev. D **84**, 052004 (2011). doi:10.1103/PhysRevD.84.052004. arXiv:1107.0163 [hep-ex]
21. C. Hanhart, YuS Kalashnikova, A.E. Kudryavtsev, A.V. Nefediev, Phys. Rev. D **85**, 011501 (2012). doi:10.1103/PhysRevD.85.011501. arXiv:1111.6241 [hep-ph]
22. D. Gamermann, E. Oset, Phys. Rev. D **80**, 014003 (2009). doi:10.1103/PhysRevD.80.014003. arXiv:0905.0402 [hep-ph]
23. B. Aubert et al. (BaBar), Phys. Rev. Lett. **102**, 132001 (2009). doi:10.1103/PhysRevLett.102.132001. arXiv:0809.0042 [hep-ex]
24. R. Aaij et al. (LHCb), Nucl. Phys. **B886**, 665 (2014). doi:10.1016/j.nuclphysb.2014.06.011. arXiv:1404.0275 [hep-ex]
25. T. Mehen, R. Springer, Phys. Rev. D **83**, 094009 (2011). doi:10.1103/PhysRevD.83.094009. arXiv:1101.5175 [hep-ph]
26. E.S. Swanson, Phys. Lett. B **598**, 197 (2004). doi:10.1016/j.physletb.2004.07.059. arXiv:hep-ph/0406080 [hep-ph]
27. A.M. Badalian, V.D. Orlovsky, YuA Simonov, B.L.G. Bakker, Phys. Rev. D **85**, 114002 (2012). doi:10.1103/PhysRevD.85.114002. arXiv:1202.4882 [hep-ph]

28. T.-H. Wang, G.-L. Wang, Phys. Lett. B **697**, 233 (2011). doi:10.1016/j.physletb.2011.02.014. arXiv:1006.3363 [hep-ph]
29. E.J. Eichten, K. Lane, C. Quigg, Phys. Rev. D **73**, 014014 (2006). doi:10.1103/PhysRevD.73.014014, doi:10.1103/PhysRevD.73.079903. arXiv:hep-ph/0511179 [hep-ph]. [Erratum: Phys. Rev. D73,079903(2006)]
30. Y. Dong, A. Faessler, T. Gutsche, V.E. Lyubovitskij, J. Phys. **G38**, 015001 (2011). doi:10.1088/0954-3899/38/1/015001. arXiv:0909.0380 [hep-ph]
31. M. Takizawa, S. Takeuchi, PTEP **2013**, 0903D01 (2013). doi:10.1093/ptep/ptt063. arXiv:1206.4877 [hep-ph]
32. F.-K. Guo, C. Hanhart, YuS Kalashnikova, U.-G. Meißner, A.V. Nefediev, Phys. Lett. B **742**, 394 (2015). doi:10.1016/j.physletb.2015.02.013. arXiv:1410.6712 [hep-ph]
33. J. Nieves, M.P. Valderrama, Phys. Rev. D **86**, 056004 (2012). doi:10.1103/PhysRevD.86.056004. arXiv:1204.2790 [hep-ph]
34. C. Hidalgo-Duque, J. Nieves, M.P. Valderrama, Phys. Rev. D **87**, 076006 (2013). doi:10.1103/PhysRevD.87.076006. arXiv:1210.5431 [hep-ph]
35. M.P. Valderrama, Phys. Rev. D **85**, 114037 (2012). doi:10.1103/PhysRevD.85.114037. arXiv:1204.2400 [hep-ph]
36. F.-K. Guo, C. Hidalgo-Duque, J. Nieves, M.P. Valderrama, Phys. Rev. D **88**, 054007 (2013). doi:10.1103/PhysRevD.88.054007. arXiv:1303.6608 [hep-ph]
37. L. Liu, G. Moir, M. Peardon, S.M. Ryan, C.E. Thomas, P. Vilaseca, J.J. Dudek, R.G. Edwards, B. Joo, D.G. Richards (Hadron Spectrum). JHEP **07**, 126 (2012). doi:10.1007/JHEP07(2012)126. arXiv:1204.5425 [hep-ph]
38. S. Prelovsek, L. Leskovec, Phys. Rev. Lett. **111**, 192001 (2013). doi:10.1103/PhysRevLett.111.192001. arXiv:1307.5172 [hep-lat]
39. S. Prelovsek, L. Leskovec, Phys. Lett. B **727**, 172 (2013). doi:10.1016/j.physletb.2013.10.009. arXiv:1308.2097 [hep-lat]
40. S. Prelovsek, C.B. Lang, L. Leskovec, D. Mohler, Phys. Rev. D **91**, 014504 (2015). doi:10.1103/PhysRevD.91.014504. arXiv:1405.7623 [hep-lat]
41. M. Padmanath, C.B. Lang, S. Prelovsek, Phys. Rev. D **92**, 034501 (2015). doi:10.1103/PhysRevD.92.034501. arXiv:1503.03257 [hep-lat]
42. M. Albaladejo, C. Hidalgo-Duque, J. Nieves, E. Oset, Phys. Rev. D **88**, 014510 (2013). doi:10.1103/PhysRevD.88.014510. arXiv:1304.1439 [hep-lat]
43. P.G. Ortega, J. Segovia, D.R. Entem, F. Fernandez, Phys. Rev. D **81**, 054023 (2010). doi:10.1103/PhysRevD.81.054023. arXiv:1001.3948 [hep-ph]
44. D.R. Entem, P.G. Ortega, F. Fernandez, *Proceedings, 16th International Conference on Hadron Spectroscopy (Hadron 2015): Newport News, Virginia, USA, September 13-18, 2015*, AIP Conf. Proc. **1735**, 060006 (2016). doi:10.1063/1.4949442. arXiv:1601.03901 [hep-ph]
45. V. Baru, E. Epelbaum, A.A. Filin, C. Hanhart, U.-G. Meißner, A.V. Nefediev (2016). arXiv:1605.09649 [hep-ph]
46. B. Grinstein, E.E. Jenkins, A.V. Manohar, M.J. Savage, M.B. Wise, Nucl. Phys. B **380**, 369 (1992). doi:10.1016/0550-3213(92)90248-A. arXiv:hep-ph/9204207 [hep-ph]
47. E.E. Jenkins, M.E. Luke, A.V. Manohar, M.J. Savage, Nucl. Phys. B **390**, 463 (1993). doi:10.1016/0550-3213(93)90464-Z. arXiv:hep-ph/9204238 [hep-ph]
48. R. Casalbuoni, A. Deandrea, N. Di Bartolomeo, R. Gatto, F. Feruglio, G. Nardulli, Phys. Lett. B **302**, 95 (1993). doi:10.1016/0370-2693(93)90641-T
49. M.T. AlFiky, F. Gabbiani, A.A. Petrov, Phys. Lett. B **640**, 238 (2006). doi:10.1016/j.physletb.2006.07.069. arXiv:hep-ph/0506141 [hep-ph]
50. A.V. Manohar, M.B. Wise, Camb. Monogr. Part. Phys. Nucl. Phys. Cosmol. **10**, 1 (2000)
51. P. Colangelo, F. De Fazio, T.N. Pham, Phys. Rev. D **69**, 054023 (2004). doi:10.1103/PhysRevD.69.054023. arXiv:hep-ph/0310084 [hep-ph]
52. T. Barnes, S. Godfrey, E.S. Swanson, Phys. Rev. D **72**, 054026 (2005). doi:10.1103/PhysRevD.72.054026. arXiv:hep-ph/0505002 [hep-ph]
53. C. Hidalgo-Duque, J. Nieves, A. Ozpineci, V. Zamiralov, Phys. Lett. B **727**, 432 (2013). doi:10.1016/j.physletb.2013.10.056. arXiv:1305.4487 [hep-ph]
54. E. Epelbaum, H.-W. Hammer, U.-G. Meißner, Rev. Mod. Phys. **81**, 1773 (2009). doi:10.1103/RevModPhys.81.1773. arXiv:0811.1338 [nucl-th]
55. V. Baru, C. Hanhart, YuS Kalashnikova, A.E. Kudryavtsev, A.V. Nefediev, Eur. Phys. J. A **44**, 93 (2010). doi:10.1140/epja/i2010-10929-7. arXiv:1001.0369 [hep-ph]
56. S. Weinberg, Phys. Rev. **130**, 776 (1993). doi:10.1103/PhysRev.130.776
57. S. Weinberg, Phys. Rev. **137**, B672 (1965). doi:10.1103/PhysRev.137.B672
58. T. Hyodo, Int. J. Mod. Phys. A **28**, 1330045 (2013). doi:10.1142/S0217751X13300457. arXiv:1310.1176 [hep-ph]
59. T. Sekihara, T. Hyodo, D. Jido, PTEP **2015**, 063D04 (2015). doi:10.1093/ptep/ptv081. arXiv:1411.2308 [hep-ph]
60. C. Garcia-Recio, C. Hidalgo-Duque, J. Nieves, L.L. Salcedo, L. Tolos, Phys. Rev. D **92**, 034011 (2015). doi:10.1103/PhysRevD.92.034011. arXiv:1506.04235 [hep-ph]
61. F. Aceti, L.R. Dai, L.S. Geng, E. Oset, Y. Zhang, Eur. Phys. J. A **50**, 57 (2014). doi:10.1140/epja/i2014-14057-2. arXiv:1301.2554 [hep-ph]
62. T. Hyodo, D. Jido, A. Hosaka, Phys. Rev. C **85**, 015201 (2012). doi:10.1103/PhysRevC.85.015201. arXiv:1108.5524 [nucl-th]
63. Z.-H. Guo, J.A. Oller, Phys. Rev. D **93**, 096001 (2016). doi:10.1103/PhysRevD.93.096001. arXiv:1508.06400 [hep-ph]
64. M. Albaladejo, F.K. Guo, C. Hidalgo-Duque, J. Nieves, M.P. Valderrama, Eur. Phys. J. C **75**, 547 (2015). doi:10.1140/epjc/s10052-015-3753-6. arXiv:1504.00861 [hep-ph]
65. J. Segovia, D.R. Entem, F. Fernandez, E. Hernandez, Int. J. Mod. Phys. E **22**, 1330026 (2013). doi:10.1142/S0218301313300269. arXiv:1309.6926 [hep-ph]
66. D. Ebert, R.N. Faustov, V.O. Galkin, Eur. Phys. J. C **71**, 1825 (2011). doi:10.1140/epjc/s10052-011-1825-9. arXiv:1111.0454 [hep-ph]
67. C. Hanhart, J.R. Pelaez, G. Rios, Phys. Lett. B **739**, 375 (2014). doi:10.1016/j.physletb.2014.11.011. arXiv:1407.7452 [hep-ph]
68. V. Baru, J. Haidenbauer, C. Hanhart, Yu. Kalashnikova, A.E. Kudryavtsev, Phys. Lett. B **586**, 53 (2004). doi:10.1016/j.physletb.2004.01.088. arXiv:hep-ph/0308129 [hep-ph]
69. F.-K. Guo, C. Hanhart, G. Li, U.-G. Meißner, Q. Zhao, Phys. Rev. D **83**, 034013 (2011). doi:10.1103/PhysRevD.83.034013. arXiv:1008.3632 [hep-ph]
70. J. Nieves, E. Ruiz Arriola, Phys. Rev. **D64**, 116008 (2001). doi:10.1103/PhysRevD.64.116008. arXiv:hep-ph/0104307 [hep-ph]
71. J. Ferretti, G. Galat, E. Santopinto, Phys. Rev. D **90**, 054010 (2014). doi:10.1103/PhysRevD.90.054010. arXiv:1401.4431 [nucl-th]
72. W. Kwong, J.L. Rosner, Phys. Rev. D **38**, 279 (1988). doi:10.1103/PhysRevD.38.279
73. L. Motyka, K. Zalewski, Eur. Phys. J. C **4**, 107 (1998). doi:10.1007/s100529800743, doi:10.1007/s100520050190. arXiv:hep-ph/9709254 [hep-ph]
74. J. Segovia, P.G. Ortega, D.R. Entem, F. Fernández, Phys. Rev. D **93**, 074027 (2016). doi:10.1103/PhysRevD.93.074027. arXiv:1601.05093 [hep-ph]